SCIENCE CHINA
Earth Sciences

• REVIEW •

November 2017 Vol.60 No.11:1976–2000
doi: 10.1007/s11430-017-9090-4

Mantle geochemistry: Insights from ocean island basalts

HUANG ShiChun[1*] & ZHENG YongFei[2]

[1] *Department of Geoscience, University of Nevada, Las Vegas, NV 89152, USA;*
[2] *CAS Key Laboratory of Crust-Mantle Material and Environment, School of Earth and Space Sciences, University of Science and Technology of China, Hefei 230026, China*

Received April 24, 2017; accepted August 4, 2017; published online October 10, 2017

Abstract The geochemical study of the Earth's mantle provides important constraints on our understanding of the formation and evolution of Earth, its internal structure, and the mantle dynamics. The bulk Earth composition is inferred by comparing terrestrial mantle rocks with chondrites, which leads to the chondritic Earth model. That is, Earth has the same relative proportions of refractory elements as that in chondrites, but it is depleted in volatiles. Ocean island basalts (OIB) may be produced by mantle plumes with possible deep origins; consequently, they provide unique opportunity to study the deep Earth. Isotopic variations within OIB can be described using a limited number of mantle endmembers, such as EM1, EM2 and HIMU, and they have been used to decipher important mantle processes. Introduction of crustal material into the deep mantle via subduction and delamination is important in generating mantle heterogeneity; however, there is active debate on how they were sampled by mantle melting, i.e., the role of olivine-poor lithologies in the OIB petrogenesis. The origin and location of high $^{3}He/^{4}He$ mantle remain controversial, ranging from unprocessed (or less processed) primitive material in the lower mantle to highly processed materials with shallow origins, including ancient melting residues, mafic cumulates under arcs, and recycled hydrous minerals. Possible core-mantle interaction was hypothesized to introduce distinctive geochemical signatures such as radiogenic ^{186}Os and Fe and Ni enrichment in the OIB. Small but important variations in some short-lived nuclides, including ^{142}Nd, ^{182}W and several Xe isotopes, have been reported in ancient and modern terrestrial rocks, implying that the Earth's mantle must have been differentiated within the first 100 Myr of its formation, and the mantle is not efficiently homogenized by mantle convection.

Keywords Mantle structure, Mantle composition, Crustal components, Crust-mantle interaction, Crustal recycling

Citation: Huang S C, Zheng Y F. 2017. Mantle geochemistry: Insights from ocean island basalts. Science China Earth Sciences, 60: 1976–2000, doi: 10.1007/s11430-017-9090-4

1. Introduction

The Earth's mantle is the dominant portion of Earth. Mantle convection provides the internal driving force shaping the Earth's surface: new crust being formed at mid-ocean ridges, arcs and backarc basins via basaltic volcanism, and oceanic crust being returned back to the mantle via subduction (Hofmann and White, 1982; Stern, 2002; Zheng and Chen, 2016). Such processes are thought to be important to life (e.g., Korenaga, 2012; Seager, 2013; Foley, 2015). For example, the climate is regulated by carbon cycle, which in turn is controlled by plate tectonics (Hilton et al., 2002; Jarrard, 2003; Dasgupta and Hirschmann, 2010). The changing environments force life to evolve continuously to fit the new living environments. Large volcanism provides essential nutrients for life, such as Zn and Cu (e.g., Kelley et al., 2002). When compared to other Solar system objects, the composition of the Earth's mantle provides important constraints on our understanding of the early Solar system formation and evolution (Anders and Grevesse, 1989; Boyet and Carlson, 2005; Huang and Jacobsen, 2017). In the past decade, NASA's Kepler telescope found many exoplanets, which led to an emerging field of exoplanet. A thorough understanding of how the Earth's mantle evolved to its current situation provides critical constraints in

* Corresponding author (email: shichun.huang@unlv.edu)

studying the possible internal structures of exoplanets (Zeng et al., 2016).

The Earth's mantle is hard to be directly sampled for geochemical studies. Consequently, most geochemical studies focus on the derivative products of the Earth's mantle, i.e., oceanic and continental basalts (Allègre, 1982; Zindler and Hart, 1986; Hofmann, 1997, 2014; Farmer, 2003). The mantle, as primarily sampled by oceanic and continental basalts, shows large chemical and isotopic variations that can be bracketed by a few end-member compositions (Zindler and Hart, 1986; Hofmann, 1997, 2014; White, 2015). The spectrum of geochemical compositions in oceanic basalts evidently reflects the large-scale geochemical heterogeneity of the Earth's mantle. Mantle melting is the primary process differentiating the silicate Earth. Together with crustal recycling, mantle metasomatism, delamination and mantle convection, they produce the observed mantle heterogeneity. However, the details about how the mantle heterogeneity has been generated in the Erath's history and to which extent it has been sampled by oceanic and continental basalts remain controversial. In this review, we try to provide an updated picture of our current understanding of the Earth's mantle, focusing on the geochemistry of ocean island basalts (OIB) with reference to mid-ocean ridge basalts (MORB), because they may sample different portions of the mantle. Tables 1–3 present a compilation of average major and trace element abundances and Sr-Nd-Hf-Pb isotope compositions in several OIB settings. Continental basalts and island arc basalts also provide clues to the mantle, but their geochemistry is highly influenced by shallow crustal components (Zheng et al., 2015; Xu and Zheng, 2017).

2. The composition of Earth, and its relationship to chondrites

Studies of seismic waves penetrating the deep interior of Earth, and the comparison of the observed seismic wave velocities within Earth with that measured in high-pressure high-temperature experiments revealed the layered structure of this planet, including a metallic core, an olivine dominated mantle, and a feldspar dominated crust (e.g., Birch, 1952; Dziewonski and Anderson, 1981). How is the composition of bulk silicate Earth, which is highly differentiated, obtained? It has been assumed for a long time that the formation of the Earth is related to the chondrite formation (e.g., Patterson, 1956), so that chondrites have been used to constrain the composition of bulk silicate Earth (e.g., Jagoutz et al., 1979; Jacobsen and Wasserburg, 1980; Palme and O'Neill, 2014). Specifically, Jagoutz et al. (1979) showed that in an Al/Si vs. Mg/Si plot, chondrites form a positive trend, whereas mantle peridotites form a negative trend (Figure 1). During nebular condensation and evaporation processes, Mg and Al are more refractory than Si (e.g., Lodders, 2003; Palme et al., 2014); consequently, the positive chondrite Al/Si vs. Mg/Si trend was interpreted to reflect "cosmochemical fractionation" (Jagoutz et al., 1979). In contrast, Drake and Righter (2002)

Table 1 Average major element compositions (in wt%) in OIB and MORB[a)]

Location	SiO_2	TiO_2	Al_2O_3	FeOT	CaO	MgO	MnO	K_2O	Na_2O	P_2O_5
Azores	46.0	2.72	13.5	10.4	11.1	10.3	0.17	1.09	2.64	0.45
Samoa	45.5	3.39	12.2	11.9	10.6	11.3	0.17	1.24	2.58	0.47
Society	45.1	3.17	11.8	11.9	10.6	11.5	0.17	1.38	2.52	0.52
Marquesas	45.3	3.21	12.3	11.8	9.8	10.8	0.18	1.08	2.47	0.45
Mascarene	46.5	2.26	13.7	11.9	10.3	10.5	0.17	0.65	2.51	0.27
Kerguelen	46.6	2.06	14.0	11.4	9.9	10.8	0.18	0.84	2.33	0.32
Pitcairn	46.4	2.95	13.3	11.3	9.6	10.5	0.16	0.80	2.49	0.45
Cook-Austral	43.3	2.71	11.6	12.2	11.8	11.5	0.19	0.95	2.68	0.53
St Helena	44.7	2.57	12.3	11.6	11.3	11.4	0.17	0.79	2.17	0.38
Cape Verde	42.2	3.64	12.1	12.0	12.4	11.6	0.19	1.04	2.57	0.67
Cameroon Line	43.6	3.33	11.9	13.2	10.6	10.7	0.19	1.38	2.84	0.81
Canary	43.6	3.36	11.8	12.2	11.0	11.1	0.18	1.07	2.85	0.69
Madeira	44.3	2.68	13.4	11.6	10.8	10.9	0.19	0.84	2.68	0.56
Selvagen	43.0	2.34	12.9	10.7	11.1	10.6	0.19	0.94	2.95	0.78
Comoros	43.7	2.44	12.1	10.3	11.7	11.3	0.20	1.01	2.90	0.56
Iceland	48.0	1.32	15.0	10.5	12.3	9.9	0.18	0.19	1.88	0.14
Galapagos	47.7	1.69	15.4	9.9	11.3	10.3	0.16	0.40	2.58	0.20
Hawaii	48.1	2.33	12.6	11.5	10.5	10.5	0.18	0.51	2.26	0.30
MORB	50.5	1.68	14.7	10.4	11.4	7.6	0.18	0.16	2.79	0.18

a) In order to minize crystal fractionation/accumulation effects, only lavas with 8%<MgO<16% are included. MORB data are all MORB mean from Gale et al. (2013) and OIB data are from GeoRoc data base.

Table 2 Average trace element compositions (in ppm) in OIB and MORB

Location	Sc	V	Cr	Ni	Cu	Zn	Ga	Rb	Sr	Y	Zr	Nb	Ba	La	Ce	Pr
Azores	28.6	265	505	198	65	93	18.8	25.4	555	25.4	209	43.2	360	31.5	65.6	7.9
Samoa	27.8	285	550	301	73	120	20.1	33.8	543	26.8	221	44.8	365	36.8	73.9	8.7
Society	23.3	263	494	315	69	129	18.6	33.6	665	28.5	276	41.5	442	37.5	83.5	10.6
Marquesas	23.7	285	503	301	59	115	20.6	27.8	597	39.3	259	40.1	328	36.0	72.6	11.0
Mascarene	28.0	267	437	286	86	104	19.3	14.1	354	25.6	147	19.8	169	16.8	36.1	4.7
Kerguelen	27.9	205	455	244	67	97	18.1	19.6	427	20.7	148	22.0	280	20.0	43.5	6.1
Pitcairn	23.5	239	377	234	58	111	19.7	15.5	483	26.2	229	28.8	216	27.1	59.1	7.7
Cook-Austral	30.4	268	513	248	87	117	17.7	23.8	663	25.4	217	52.7	396	40.4	82.2	8.8
St Helena	35.1	237	566	251	70	93		14.5	460	22.0	185	40.5	228	28.1	59.7	7.0
Cape Verde	27.9	325	526	256	67	119	20.0	24.2	824	27.7	262	66.4	604	46.6	93.3	12.3
Cameroon Line	26.1	275	414	282	51	123		34.4	848	31.0	302	59.8	566	54.8	113.3	
Canary	29.3	299	502	277	93	114	20.4	22.5	747	27.1	264	58.3	401	56.6	96.0	13.6
Madeira	29.7	315	540	239	67	101	18.6	19.4	606	28.4	225	48.2	282	38.0	77.2	9.4
Selvagen		248	415	307		117	17.9	19.9	795	26.5	202	61.4	479	53.5	106.9	12.1
Comoros	27.6	256	507	283	77	105	18.5	32.0	641	27.2	193	61.3	570	50.6	94.2	11.1
Iceland	40.4	276	477	192	119	81	14.9	6.2	170	20.8	72	9.7	54	6.2	15.1	2.1
Galapagos	33.7	250	509	243	86	81	18.7	8.2	316	24.1	116	14.2	115	10.0	22.1	2.8
Hawaii	27.8	273	556	299	93	117	18.4	10.6	423	25.3	144	20.0	234	18.0	38.0	5.1
MORB	39.8	309	249	92	74	91	17.5	2.88	129	36.8	117	5.24	29.2	5.21	14.9	2.24

Location	Nd	Sm	Eu	Gd	Tb	Dy	Ho	Er	Tm	Yb	Lu	Hf	Ta	Pb	Th	U
Azores	34.2	7.19	2.33	6.56	0.95	5.17	0.91	2.38	0.324	1.99	0.275	4.91	2.83	2.43	3.24	0.99
Samoa	37.2	8.16	2.58	7.52	1.07	5.79	1.01	2.44	0.308	1.79	0.253	5.60	2.94	3.45	4.34	1.02
Society	45.7	9.29	3.06	8.34	1.13	6.04	0.99	2.45	0.320	1.82	0.258	6.66	2.63	3.88	5.14	1.40
Marquesas	41.9	9.12	2.92	9.58	1.24	7.62	1.28	3.55	0.958	2.37	0.322	6.03	2.89	5.00	4.27	1.01
Mascarene	21.0	4.96	1.69	5.20	0.82	4.65	0.88	2.30	0.304	1.90	0.275	3.59	1.16	2.08	2.03	0.46
Kerguelen	23.2	4.96	1.66	4.99	0.72	4.27	0.81	2.11	0.249	1.67	0.237	3.57	1.53	1.77	2.48	0.46
Pitcairn	31.5	7.25	2.29	6.65	0.93	5.26	0.92	2.47	0.328	1.85	0.256	5.37	2.16	2.85	2.81	0.70
Cook-Austral	39.4	7.75	2.49	6.71	1.02	5.18	0.90	2.33	0.284	1.72	0.245	4.95	3.08	2.75	4.90	1.12
St Helena	29.9	6.26	2.05	5.91	0.87	4.59	0.85	2.21	0.284	1.73	0.242	4.50	2.38	1.49	3.06	0.85
Cape Verde	48.3	10.0	3.16	8.73	1.23	5.93	1.02	2.51	0.323	1.88	0.264	6.78	4.73	2.23	4.19	1.29
Cameroon Line	55.9	11.9												3.19	6.89	1.47
Canary	49.0	10.3	3.17	9.10	1.21	6.07	1.04	2.52	0.317	1.86	0.251	5.63	3.39	3.34	5.78	1.28
Madeira	38.4	7.90	2.55	7.65	1.07	5.98	1.11	2.83	0.363	2.08	0.297	5.39	2.81	1.90	3.79	0.98
Selvagen	45.4	8.88	2.67	7.74	1.23	5.46	0.95	2.35	0.286	1.75	0.240	4.72	3.33	3.31	5.62	6.71
Comoros	40.9	7.98	2.45	7.03	0.99	5.24	0.93	2.37	0.340	1.87	0.266	4.51	3.94	3.53	6.26	1.30
Iceland	9.8	2.70	1.01	3.21	0.55	3.40	0.70	1.99	0.293	1.89	0.288	2.22	0.79	0.93	0.64	0.23
Galapagos	12.9	3.57	1.29	4.14	0.70	4.28	0.89	2.42	0.349	2.13	0.330	2.49	1.04	1.24	0.96	0.22
Hawaii	23.1	5.82	1.96	5.84	0.88	4.93	0.91	2.29	0.308	1.81	0.257	3.52	1.43	1.46	1.61	0.41
MORB	12.0	3.82	1.36	4.99	0.90	6.08	1.28	3.79		3.63	0.53	2.79	0.34	0.57	0.404	0.119

described this trend as an "unexplained trend". The negative peridotite Al/Si vs. Mg/Si trend reflects the effect of partial melting, because Al is incompatible whereas Mg is compatible during mantle melting (e.g., Kushiro, 2001). The chemical composition of bulk silicate Earth is suggested at the intersection of these two trends (Jagoutz et al., 1979), and the refractory element pattern of the Earth is similar to that in chondrites (Jacobsen and Wasserburg, 1980; Sun, 1982; McDonough and Sun, 1995). This is the so-called chondritic Earth model. It should not be mistaken as that the bulk silicate Earth has the average composition of chondrites. It has been known for several decades that the bulk silicate Earth is depleted in volatiles, such as K, relative to chondrites (e.g., Figure 2).

Table 3 Average radiogenic isotopic compositions in OIB and MORB

Location	$^{143}Nd/^{144}Nd$	$^{87}Sr/^{86}Sr$	$^{206}Pb/^{204}Pb$	$^{207}Pb/^{204}Pb$	$^{208}Pb/^{204}Pb$	$^{176}Hf/^{177}Hf$
Azores	0.512884	0.703771	19.642	15.629	39.363	0.282969
Samoa	0.512749	0.705603	18.995	15.603	39.184	0.282938
Society	0.512793	0.704616	19.077	15.585	38.792	0.282952
Marquesas	0.512841	0.704201	19.220	15.582	39.067	0.282992
Mascarene	0.512884	0.703929	18.854	15.584	38.923	0.283056
Kerguelen	0.512678	0.705326	18.333	15.541	38.831	0.282865
Pitcairn	0.512764	0.703948	18.512	15.528	38.954	0.282939
Cook-Austral	0.512839	0.703311	20.267	15.692	39.739	0.282916
St Helena	0.512901	0.702884	20.625	15.757	39.947	0.282885
Cape Verde	0.512836	0.703336	19.429	15.589	39.118	0.282923
Cameroon Line	0.512904	0.703271	19.427	15.637	39.275	0.282930
Canary	0.512911	0.703144	19.483	15.587	39.255	0.283002
Madeira	0.513068	0.702819	19.192	15.539	38.856	0.283251
Selvagen	0.512917	0.703105	19.460	15.575	39.263	0.283035
Comoros	0.512816	0.703421	19.478	15.599	39.333	
Iceland	0.513044	0.703178	18.451	15.464	38.093	0.283198
Galapagos	0.513006	0.703142	19.030	15.563	38.656	0.283108
Hawaii	0.512974	0.703548	18.260	15.463	37.946	0.283096
MORB	0.513074	0.702819	18.412	15.515	38.100	0.283164

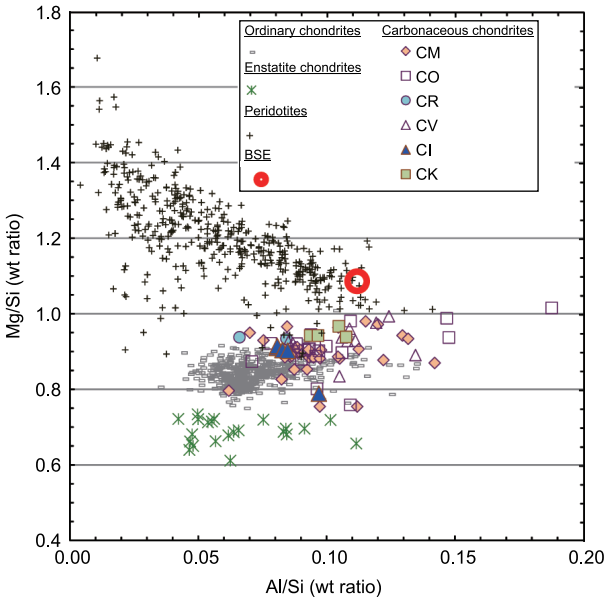

Figure 1 Plot of Al/Si vs. Mg/Si for chondrites and peridotites. Chondrite data are from the compilation of Nittler et al. (2004), terrestrial peridotite data are from GeoRoc database, and bulk silicate Earth (BSE) estimate is from McDonough and Sun (1995).

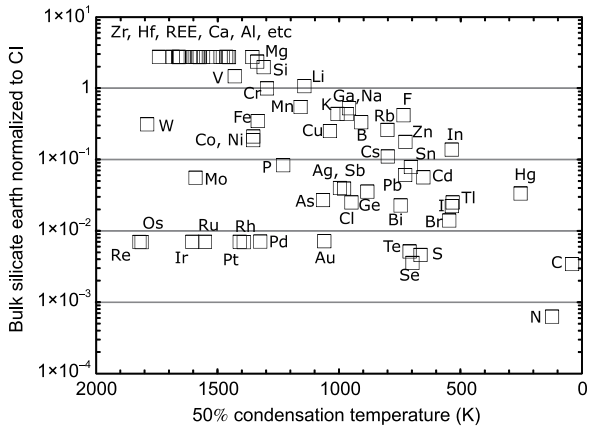

Figure 2 Bulk silicate Earth composition normalized to CI chondrite composition (McDonough and Sun, 1995) plotted against their 50% condensation temperatures at 10^{-4} bar total pressure in a nebula with the Solar composition (Lodders, 2003).

Although carbonaceous chondrites seem the closest match to the bulk silicate Earth in terms of chemical compositions (e.g., Figure 1), they differ most in isotopic compositions. For example, in a three oxygen isotope plot, enstatite chondrites have essentially the same O isotopic compositions as Earth (Figure 3), but carbonaceous chondrites are very different from Earth (Clayton, 2003). In fact, compared to Earth, carbonaceous chondrites show nucleosynthetic anomalies in many elements, such as ^{26}Al (Lee et al., 1976), Ca (Lee et al., 1978; Jungck et al., 1984; Simon et al., 2009; Chen et al., 2011; Dauphas et al., 2014; Huang and Jacobsen, 2017), Ti (Niederer et al., 1985; Zhang et al., 2012), Mo (Yin et al., 2002), and Os (Brandon et al., 2005), which may be related to the abundant Ca-Al-rich inclusions in carbonaceous chondrites (e.g., Niederer and Papanastassiou, 1984; Huang et al., 2012). Consequently, carbonaceous chondrites may provide

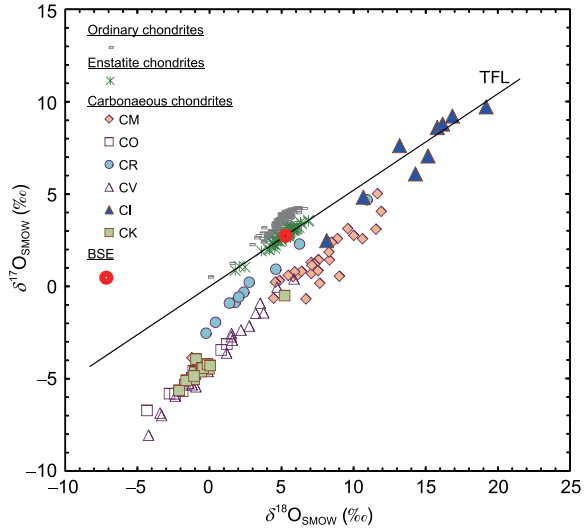

Figure 3 Three oxygen isotope plot. Data are from Clayton et al. (1991), Clayton and Mayeda (1999), and Newton et al. (2000).

a good constraint on the chemical compositions of bulk silicate Earth, but they are not suitable for constraining the isotopic compositions of Earth.

The recent debate on the non-chondritic Earth model (Boyet and Carlson, 2005; Campbell and O'Neill, 2012), in fact, originates from using carbonaceous chondrites as the reference point for the isotopic compositions of bulk silicate Earth. Specifically, Boyet and Carlson (2005) found that carbonaceous chondrites have $^{142}Nd/^{144}Nd$ ratios about 20 ppm lower than those of terrestrial samples (Figure 4). Since ^{142}Nd is the decay product of the now extinct short-lived ^{146}Sm with a half-life of 68 to 103 Myr (Meissner et al., 1987; Kinoshita et al., 2012), this difference may be interpreted as: (1) the nucleosynthetic ^{146}Sm or ^{142}Nd anomaly variation in the early Solar System (e.g., Ranen and Jacobsen, 2006; Andreasen and Sharma, 2006; Huang et al., 2013); (2) different Sm/Nd ratios for bulk silicate Earth and chondrites (e.g., Caro et al., 2008; Caro and Bourdon, 2010; Jackson et al., 2010; Jackson and Carlson, 2011; Jackson and Jellinek, 2013; Zhang, 2014; Jellinek and Jackson, 2015); and (3) that the bulk silicate Earth has a chondritic Sm/Nd ratio, but the accessible portion of the Earth has a higher Sm/Nd ratio than the chondritic value due to the presence of an early formed (hidden or lost) reservoir (e.g., Boyet and Carlson, 2005; Campbell and O'Neill, 2012). The origin of the ^{142}Nd difference between Earth samples and chondrites and its inference on the isotopic compositions of bulk silicate Earth have been one of the biggest debates in mantle geochemistry for the past decade.

Consequent studies of chondrites show large nucleosynthetic anomalies (Figure 4), and in most cases carbonaceous chondrites have the largest nucleosynthetic anomalies compared to the Earth (e.g, Bouvier and Boyet, 2016; Burkhardt et al., 2016). A similar case was demonstrated by O isotopes

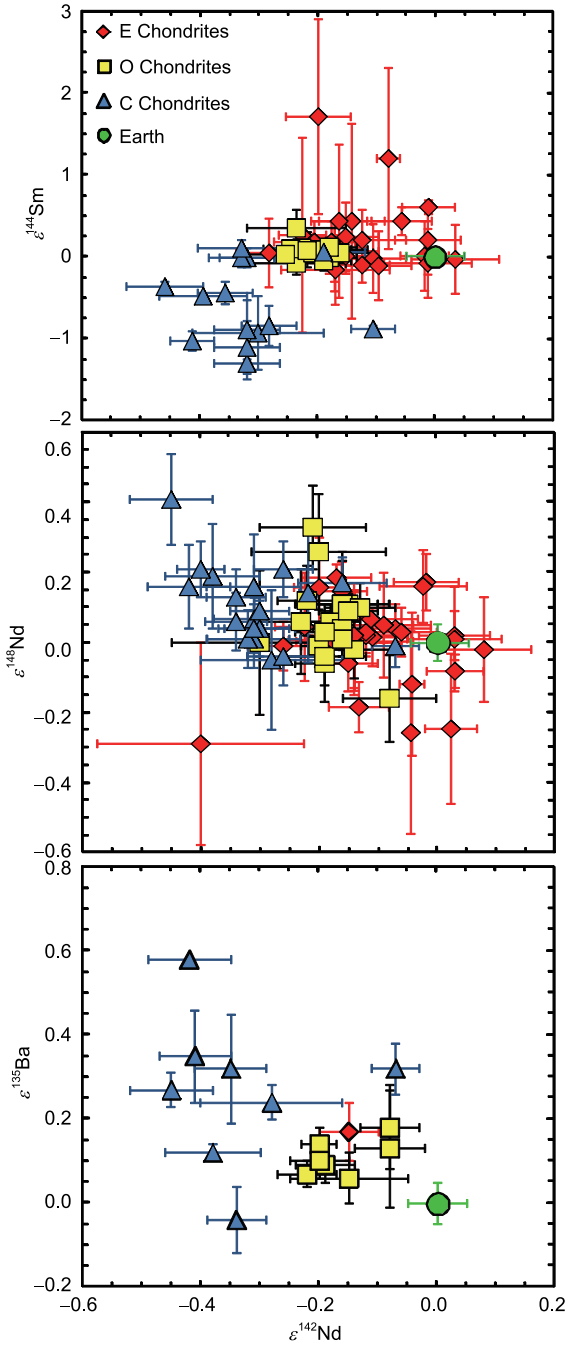

Figure 4 $\varepsilon^{142}Nd$ vs. $\varepsilon^{144}Sm$, $\varepsilon^{148}Nd$ and $\varepsilon^{135}Ba$ in bulk chondrites. Data are from Boyet and Carlson (2005), Andreasen and Sharma (2006), Carlson et al. (2007), Gannoun et al. (2011) and Burkhardt et al. (2016).

in the 1970s (Figure 3). It has been shown that Earth and enstatite chondrites have very similar $^{142}Nd/^{144}Nd$ ratios, and the observed 20 ppm difference in $^{142}Nd/^{144}Nd$ between Earth and carbonaceous chondrites reflects the nucleosynthetic anomaly, i.e., a higher proportion of s-process isotopes, including ^{142}Nd and ^{144}Sm, in the Earth (e.g, Gannoun et al., 2011; Bouvier and Boyet, 2016; Burkhardt et al., 2016). Gale et al. (2013) re-calculated the compositions of global average MORB and inferred that MORB source has Sm/Nd

and $^{143}Nd/^{144}Nd$ ratios overlapping with the proposed compositions of "bulk silicate Earth" under the superchondritic Earth model (Jackson et al., 2010; Jackson and Carlson, 2011; Jackson and Jellinek, 2013; Jellinek and Jackson, 2015) or the EDR (early depleted reservoir), which is the accessible portion of the Earth (Boyet and Carlson, 2005). Consequently, "there is no possibility of a complementary relationship between continental crust and oceanic upper mantle" under the superchondritic Earth model (Gale et al., 2013). Using published isotope dilution Sm-Nd abundance data only, Huang et al. (2013) reconstructed the crust-mantle ^{147}Sm-^{143}Nd systematics, and their mass balance calculations suggest that the bulk silicate Earth, or the accessible portion of Earth, has a chondritic Sm/Nd ratio, consistent with the isotopic studies of chondrites.

3. The structure of mantle: layered mantle convection vs. whole mantle convection

The Earth has a layered structure of core, mantle, and crust, as imaged by seismic waves (Dziewonski and Anderson, 1981). There are two global seismic wave velocity discontinuities within the mantle at the depths of 410 and 660 km, respectively, corresponding to phase changes from olivine to wadsleyite, and ringwoodite to bridgmanite and periclase. The 660 km discontinuity was considered a barrier for whole mantle convection, and layered mantle convection, two isolated convection cells separated by the 660 km discontinuity, was popular in the last century (Figure 5a). The seismic finding that some slabs can penetrate the 660 km discontinuity (van der Hilst et al., 1997) challenged this traditional model of two-layered mantle convection. Mass exchange across the 660 km discontinuity is allowed in the whole mantle convection model (Figure 5b). So does a hybrid model in which mantle convection rates in the upper and lower mantle are different (Figure 5c), and the mass exchange between the upper and lower mantle is limited (Gonnermann and Mukhopadhyay, 2009).

Bercovici and Karato (2003) hypothesized that the mantle transition zone acts as a filter for water and other highly incompatible elements due to dehydration melting. Specifically, the mantle transition zone minerals, wadsleyite and ringwoodite, have a much higher water solubility than the upper mantle mineral, olivine, and lower mantle minerals, bridgmanite and periclase. As a consequence, when the upwelling mantle flow passes through the 410 km boundary, water dissolved in wadsleyite becomes a free phase because of the much lower olivine water solubility, which, in turn, leads to dehydration melting of the mantle. Similarly, when the downwelling mantle flow passes through the 660 km boundary, dehydration melting also occurs due to the phase transition of ringwoodite to bridgmanite and periclase (Schmandt et al., 2014). The net effect is that both the upwelling and downwelling mantle flows through the mantle transition zone are likely to undergo dehydration melting at the 410 and 660 km boundaries, respectively, which will deplete the water and other highly incompatible elements in the mantle flows that leave the mantle transition zone. So that even under a whole mantle convection scenario, the upper and lower mantle may have different compositions, and the mantle transition zone may be water-rich.

Isotopic variations in oceanic basalts have been observed probably since Gast et al. (1964), and Hart (1971) showed that MORB and OIB are characterized by different K/Rb and $^{87}Sr/^{86}Sr$ ratios. For example, despite significant overlap, MORB tend to have less variable, lower $^{87}Sr/^{86}Sr$ and higher $^{143}Nd/^{144}Nd$ ratios than OIB (Figure 6). In particular, MORB are depleted in highly incompatible trace elements such as large ion lithophile elements (LILE) and light rare earth elements (LREE) relative to OIB. Recent high precision isotopic data on noble gas isotopes, Ne and Xe, also reveal a difference between MORB and OIB (Mukhopadhyay, 2012). The isotopic difference between MORB and OIB evidently requires different mantle sources (e.g., Zindler and Hart, 1986; Hofmann, 1997); however, the physical locations of MORB and OIB sources cannot be placed by geochemical data. The layered mantle convection model has been used to explain the observed geochemical difference between MORB and OIB (Figure 6). The mantle plume hypothesis (Morgan, 1971), which followed Wilson (1963), was used to explain the age progression along hot spot tracks such as Hawaii. Under the plume hypothesis, OIB may be produced by partial melting of a specific mantle material, which may rise from the lower mantle, either from the 660 km discon-

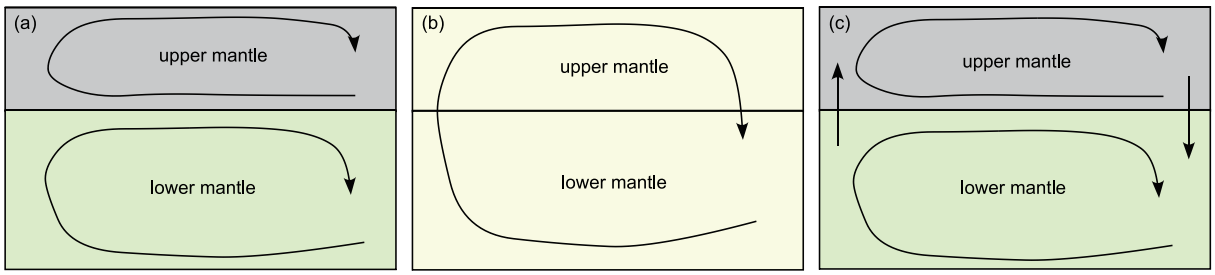

Figure 5 Cartoons of mantle convection. (a) Layered mantle convection; (b) whole mantle convection; (c) hybrid model in which upper and lower mantle are separated but with limited material exchange.

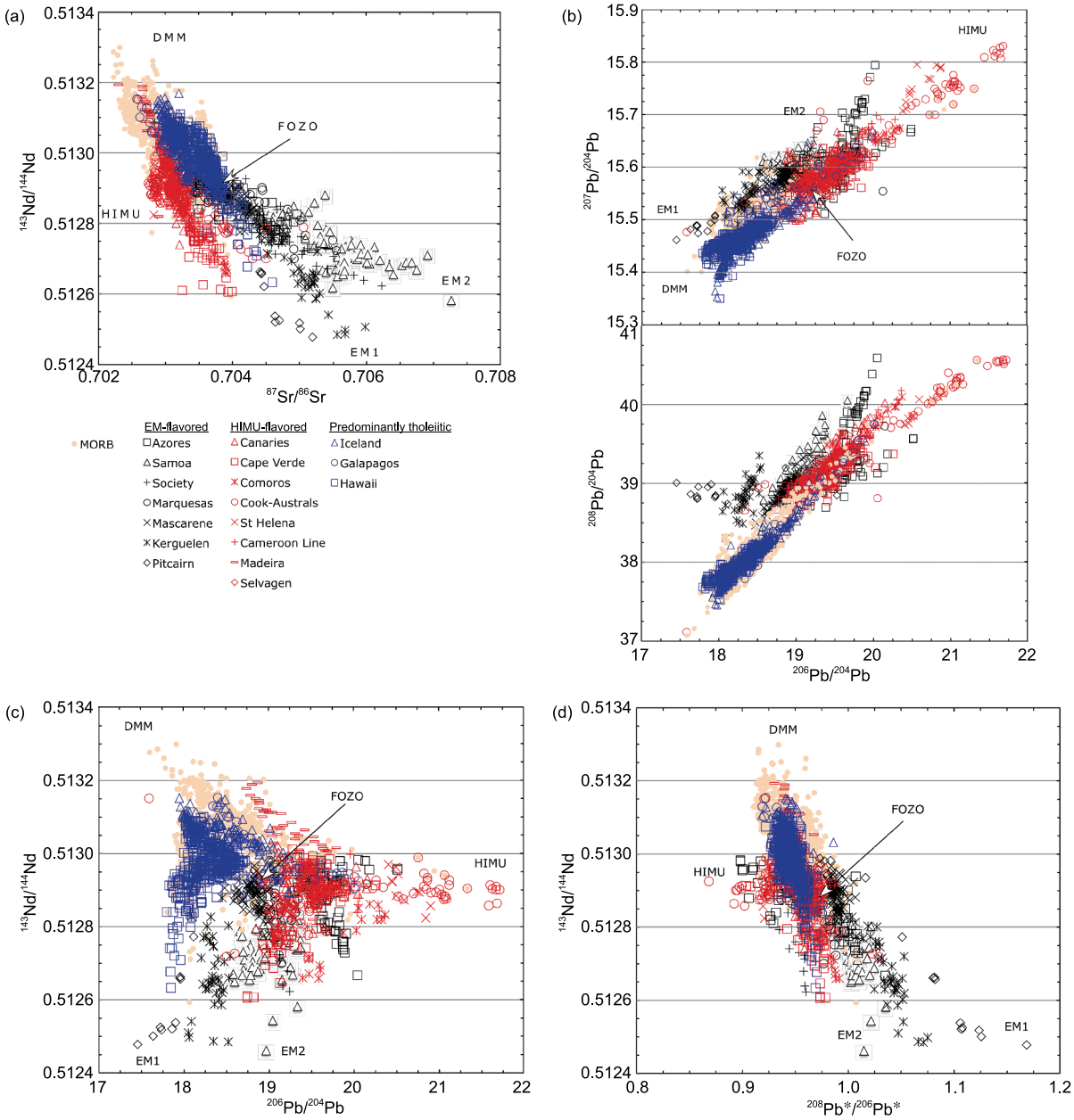

Figure 6 Sr-Nd-Pb isotopic systematics in oceanic basalts. Data are from GeoRoc and PeTDB databases.

tinuity or even from the core-mantle boundary (Morgan, 1971), and contain recycled oceanic crust (e.g., Hofmann and White, 1982).

A lower mantle origin of mantle plumes was originally hypothesized to explain the relatively fixed hotspots (Morgan, 1971); however, hotspots may move in the Earth's history. For example, Tarduno et al. (2003) measured the paleolatitudes of Hawaiian-Emperor lavas, and concluded that the Hawaiian hotspot moved southward rapidly at a speed of 40 mm a^{-1} between 81 to 47 Ma (but see Gordon and Morgan, 2016 for a different opinion). Nevertheless, under the deep plume hypothesis, the OIB sources are in the deep lower mantle, and MORB apparently sample the shallow upper mantle. Consequently, the isotopic difference between OIB and MORB is interpreted to reflect a compositional difference between the lower and upper mantle. Under this hypothesis, the lower and upper mantle remain relatively isolated throughout the Earth's history, and the mass exchange, if any, between the lower and upper mantle is very limited in the history of Earth. For instance, it was estimated that the current global hotspot buoyancy flux is 50 Mg s^{-1} (Sleep, 1990). If this flux remains the same for the whole Earth's history, the total mass transported from the lower mantle to the upper mantle is 7×10^{21} kg, which is negligible compared to the Earth's mass (6×10^{24} kg). However, the mass exchange between the lower and upper mantle may be not negligible in view of the whole mantle

convection in the history of Earth.

Historically, basalt $^{3}He/^{4}He$ ratios played an important role in supporting the mantle plume model (Figure 7). After the Earth's accretion, only ^{4}He is being made through α-decay (mostly from U and Th) on the Earth. Since He is a gas and highly incompatible during partial melting, any mantle process will decrease mantle He/(U+Th) ratios, with time leading to low $^{3}He/^{4}He$ ratios. Consequently, a primitive or less degassed mantle was supposed to have high $^{3}He/^{4}He$ ratios. The early finding that some OIB have $^{3}He/^{4}He$ higher than MORB (e.g., Kurz et al., 1982) has been used to argue that the OIB sources, mantle plumes, reside in the lower mantle, which are primitive or less degassed. Consistent with this interpretation, Lee et al. (2010) proposed that undegassed magmas formed during the first 1.0 Ga of the Earth's history now piled at the core-mantle boundary are also characterized by high $^{3}He/^{4}He$ ratios because of their high density. However, later studies show that $^{3}He/^{4}He$ ratios are more variable in OIB than MORB (Figure 7), and they range from values lower than MORB average to higher (e.g., Barfod et al., 1999). More recently, Jackson et al. (2017) argued that high $^{3}He/^{4}He$ mantle may be denser, and hence they may remain isolated from convecting mantle to keep its distinctive $^{3}He/^{4}He$ signature.

On the other hand, Parman et al. (2005) argued that during partial melting He may be more compatible than U and Th; consequently, melting residues may be characterized by high

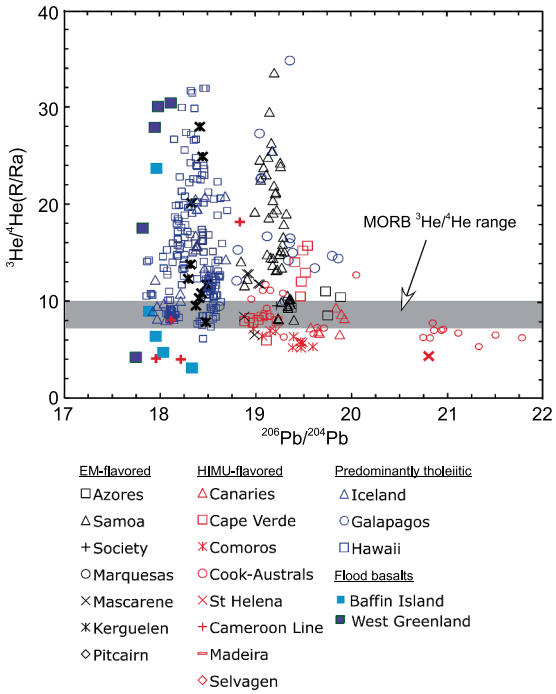

Figure 7 $^{206}Pb/^{204}Pb$ vs. $^{3}He/^{4}He$ in oceanic basalts. Data are from the compilation of Huang et al. (2013) using GeoRoc database. Some Baffin Island picrites have $^{3}He/^{4}He$ up to 50 (Stuart et al., 2003); however, because the lack of Pb isotope data on the same samples, they are not plotted.

He/(U+Th) ratios despite their low He abundance. If aged, they are expected to have high $^{3}He/^{4}He$ ratios. Along this line, Jackson et al. (2013) found that noble gases are highly soluble in amphibole, which has large unoccupied A-sites. Subducted crustal rocks are generally rich in hydrous minerals which similar to amphibole also have large A-sites, and may also be characterized by high He/(U+Th). Because hydrous minerals may be metastable at deep subduction zones (Zheng et al., 2016), it is possible for them to carry recycled noble gases into the deep mantle. As another hypothesis, sulfide-bearing cumulates formed beneath volcanic arcs during continental growth may be characterized by high He/(U+Th) because He is soluble in sulfide (Huang et al., 2014). Hence if formed early in the Earth's history, these materials can also be characterized by high $^{3}He/^{4}He$. These alternative interpretations imply that the high $^{3}He/^{4}He$ mantle source may be depleted in noble gases, which conflict with the hypothesis that high $^{3}He/^{4}He$ mantle sources may be more gas rich than MORB source (Mukhopadhyay, 2012; Tucker and Mukhopadhyay, 2014). In summary, Therefore, it is unlikely that the high $^{3}He/^{4}He$ signature can be used as a distinctive indicator for a lower mantle origin.

The upper mantle has been well sampled by MORB, so its composition is well constrained (Salters and Stracke, 2004; Workman and Hart, 2005; Gale et al., 2013; Dalton et al., 2014). If the continental crust is compositionally complementary to the upper mantle (Hofmann, 1988), the volume of the upper mantle can be estimated. For example, the ^{147}Sm-^{143}Nd systematics of the upper mantle and continental crust shows that only 25% of the whole mantle (Figure 8), which is slightly smaller than the upper mantle above the 660 discontinuity, has been processed to yield the continental crust and the rest remains primitive or unprocessed (Caro and Bourdon, 2010). In this case, the lower and upper mantle would have different geochemical compositions if they could have remained relatively isolated with each other throughout the Earth's history (Figure 5), i.e., a layered mantle convection or a hybrid model in which convection is on both layered and whole mantle scales but the mass flux through the 660 km discontinuity is limited (Gonnermann and Mukhopadhyay, 2009). In addition, terrigenous material may be carried into the mantle via plate subduction and lithospheric delamination (Armstrong, 1968; Anderson, 2005), which may complicate this mass balance approach (e.g., Jackson et al., 2007; Cabral et al., 2013), because the subducted crustal rocks could cumulate at the base of the mantle or the 660 km discontinuity. In this case, the depleted mantle volume inferred based on the current continental volume (Figure 8) is the minimum. As such, the history of continental growth (e.g., Jacobsen, 1988; Hawkesworth et al., 2016; Tang et al., 2016) is important in understanding the mantle structure.

Based on the comparison of observed lower mantle S wave

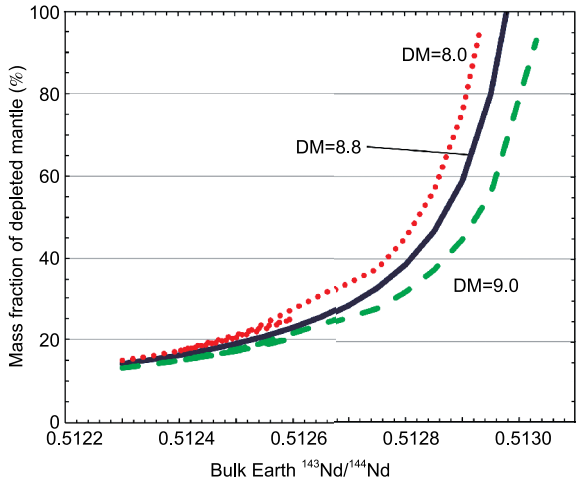

Figure 8 The mass fraction of depleted mantle as a function of bulk Earth $^{143}Nd/^{144}Nd$ under a three-reservoir model, in which the depleted mantle is complementary to the continent crust. Under the chondritic Earth model, in which bulk Earth $^{143}Nd/^{144}Nd$=0.512638, 25% of the mantle needs to be depleted to produce the continent crust. Under the super chondritic Earth model, in which bulk Earth $^{143}Nd/^{144}Nd$=0.5130, the whole mantle needs to be depleted to produce the continental crust. Model calculation inputs are: $(^{143}Nd/^{144}Nd)_{DM}$=0.51309 (Huang et al., 2013); $(^{143}Nd/^{144}Nd)_{CC}$=0.51177 (Jacobsen, 1988); $(^{143}Nd/^{144}Nd)_{PM}$=0.512638 (Jacobsen and Wasserburg, 1984); $[Nd]_{CC}$=20 ppm (Rudnick and Gao, 2003); $[Nd]_{PM}$=1.189 (Hofmann, 1988).

velocity and model results based on the laboratory determination of S wave velocities of bridgmanite and ferropericlase, it has been suggested that the lower mantle might be Si-rich compared to the upper mantle (Murakami et al., 2012). This claim to some extent is favored by the so-call "enstatite chondritic Earth" model by Javoy et al. (2010), who based on the isotopic similarity between Earth and enstatite chondrites (Figure 3), argued that the Earth is made of enstatite chondrites. However, enstatite chondrites have too much Si compared to the Earth's upper mantle (Figure 1). If the lower mantle is relatively enriched in Si, this might leverage the Si problem in the "enstatite chondritic Earth" model. Zhang et al. (2013) used the first principles calculation to investigate the elastic properties of bridgmanite ($MgSiO_3$) under lower mantle conditions, and they found lower shear moduli for bridgmanite than that reported by Murakami et al. (2012). Hyung et al. (2016) noted that Al and Ca were not considered in the original model calculation by Murakami et al. (2012). Specifically, Al affects the Fe-Mg exchange between bridgmanite and ferropericlase, and Ca requires a Ca-bearing phase that is Ca-perovskite under the lower mantle *P-T* conditions. If such minor elements are taken into account, the observed lower mantle S wave velocity structure can be reconstructed using the upper mantle composition (Zhang et al., 2013; Hyung et al., 2016). That is, the lower and upper mantle may have the same major element composition. This favors the whole mantle convection rather than the layered mantle convection.

4. Mantle heterogeneity: radiogenic isotopes and their relations to major and trace element compositions

Both MORB and OIB are heterogeneous in their radiogenic isotopic compositions of Sr, Nd, Hf, Pb and He (Figure 6), and the earliest documentation may be tracked back to Gast et al. (1964). This topic has been extensively studied in past five decades (see reviews by Zindler and Hart, 1986; Hofmann, 1997; Stracke et al., 2005; White, 2015). As advocated by Zindler and Hart (1986), the Sr, Nd, Hf, Pb and He isotopic variations in oceanic basalts may be described by several mantle endmembers such as high μ (HIMU, $\mu=^{238}U/^{204}Pb$), enriched mantle I (EM1), enriched mantle II (EM2) and depleted MORB mantle (DMM) (Figure 6). In addition, the oceanic basalts define a highly correlated $^{176}Hf/^{177}Hf$ vs $^{143}Nd/^{144}Nd$ trend called the "terrestrial array" (see Figure 1 of Vervoort et al., 1999, 2011); consequently, $^{176}Hf/^{177}Hf$ by itself does not define any mantle endmember. However, any deviation from this terrestrial array yields important constraints on its source compositions (e.g., Blichert-Toft et al., 1999; Bizimis et al., 2005; Salters et al., 2011).

The HIMU represents a high U/Pb component in the mantle source of oceanic basalts, because it is characterized by high $^{206}Pb/^{204}Pb$ (Figure 6). It is also characterized by low $^{87}Sr/^{86}Sr$ that are slightly higher than those of depleted MORB, and plots below the so-called Nd-Sr mantle array (Figure 6a, Zindler and Hart, 1986; Hauri and Hart, 1993). It has generally been considered to represent recycled, altered basaltic oceanic crust that preferentially gained water-soluble trace elements such as K, Rb, U and Pb during seawater-hydrothermal alteration at ocean ridges (Zindler et al., 1982; Chauvel et al., 1992; Hofmann, 1997; Hanyu et al., 2011). In favor of this argument, Parai et al. (2009) found that HIMU lavas from Cook-Austral islands with $^{206}Pb/^{204}Pb>20$ have low $^{3}He/^{4}He$ (<10 R/Ra), consistent with addition of ancient U-bearing material to their mantle source. Because altered oceanic basalts are relatively enriched in U, they can produce high U melts because U is incompatible. Therefore, HIMU represents the crustal signature form subducted basaltic oceanic crust.

Nevertheless, Pb isotopes in MORB do not trend towards HIMU values, so HIMU is unlikely formed directly from MORB (Hofmann, 1997; Stracke, 2012). However, this may be caused by very low Pb abundances in fresh MORB. In contrast, altered MORB are enriched in Pb and other water-soluble trace elements from seawater-hydrothermal fluids. Although these water-soluble trace elements may be lost through metamorpohic dehydration during subduction, Pb abundances in MORB-transformed eclogites are still higher than those in the fresh MORB. More importantly, low-degree melting of the eclogite makes its derived melts

with elevated Pb abundances again. Such melts would chemically react with the peridotite to generate the olivine-poor pyroxenites (silica-deficient), which may serve as the mantle sources of HIMU-type basalts.

On the other hand, minor and trace elements in olivine phenocrysts of HIMU-type basalts from Mangaia and Tubuai in the Cook-Austral Islands indicate that their mantle sources are primarily ancient subcontinental lithospheric mantle that was metasomatized by subduction-related carbonatite (Weiss et al., 2016). In this regard, the subduction-related carbonatite is relatively enriched in U, consistent with preferential partition of U into carbonatitic melt than peridotite (Dasgupta et al., 2009). This model is also consistent with the relatively low $^{87}Sr/^{86}Sr$ in HIMU lavas (Figure 6). As shown in Figure 2 of Weiss et al. (2016), the estimated HIMU-type mantle source, a mixture of depleted peridotite and carbonatite-metasomatized peridotote, has a near-primitive mantle Rb/Sr ratio.

The EM1 and EM2 are two enriched components in the mantle source of oceanic basalts, which are thought to contain recycled crustal components such as pelagic and terrigenous sediments, oceanic and continental magmatic rocks, and metamorphic granulite (e.g., Zindler and Hart, 1986; Weaver, 1991; Hofmann, 1997; Blichert-Toft et al., 1999). The EM1 signature is generally linked to the magmatic rocks of oceanic crust and the lower continental crust of ancient age. For example the lower continental crust is dominated by granulites that have low U/Pb, Th/Pb and Sm/Nd (e.g., Mansur et al., 2014) because of plagioclase and clinopyroxene accumulation. If the lower continental crust is of ancient age, its melting residues tend to have unradiogenic Pb and Nd isotope ratios. If such residues would be incorporated into the mantle sources by delamination, the resulted OIB may exhibit EM1-like Pb and Nd isotope compositions (Figure 6c; Frey et al., 2016). The EM2 signature is linked to the upper continental crust and terrigenous sediment. Specifically, Jackson et al. (2007) found very high $^{87}Sr/^{86}Sr$ (>0.72) and low $^{143}Nd/^{144}Nd$ in EM2-type lavas from Samoa, providing strong evidence for recycling of the ancient continental crust into the mantle source.

The DMM represents a depleted component in the mantle source of oceanic basalts. It is characterized by low $^{87}Sr/^{86}Sr$ and high $^{143}Nd/^{144}Nd$ in MORB (Figure 6). However, it still remains to be resolved whether the DMM in OIB is exactly the same as that sampled by normal MORB. For example, based on the geochemical similarities, Blichert-Toft and White (2001) argued that the depleted component in Galapagos lavas is the normal MORB mantle. In contrast, at Iceland, Fitton et al. (1997, 2003) argued that Icelandic depleted lavas have higher ε_{Hf} at a given ε_{Nd} than normal MORB and are enriched in Nb than the MORB, and thus they sampled a depleted non-MORB component, a point of view also shared by Chauvel and Hémond (2000). Regelous et al. (2003) and Frey et al. (2005) argued based on precise Pb isotope data that the depleted component in Hawaiian lavas is not related to MORB. At Ninetyeast Ridge in the eastern Indian Ocean, the depleted component in OIB is suggested to be ancient melting residue containing both garnet and clinopyroxene, and is not related to the source of modern MORB (Frey et al., 2015). Recycled ancient melting residues have also been argued to play an important role in generating the depleted component in Hawaiian rejuvenated stage lavas/xenoliths (Bizimis et al., 2005, 2013) and OIB in general (Salters et al., 2011) based on radiogenic $^{176}Hf/^{177}Hf$ at a given $^{143}Nd/^{144}Nd$. In this context, significant extraction of melts from crustal and mantle rocks has also contributed to the isotopically depleted signature in the oceanic basalts.

The FOZO was proposed by Hart et al. (1992) as a common component in the mantle source of oceanic basalts, and it is generally characterized by high $^{3}He/^{4}He$ and $^{143}Nd/^{144}Nd$ ratios. It is equivalent to the PHEM (primitive He mantle) by Farley et al. (1992), C by Hanan and Graham (1996) and PREMA (prevalent mantle) by Wörner et al. (1986). In detail, the FOZO is a model component rather than an endmember for most OIB and MORB arrays (Stracke et al., 2005). Its high $^{3}He/^{4}He$ was hypothesized to originate from a less processed mantle source, which is consistent with its high $^{143}Nd/^{144}Nd$, with ε_{Nd} of +7 (Jackson and Carlson, 2011). If the Earth has a superchondritic Sm/Nd ratio, ~6% higher than chondritic Sm/Nd, as inferred based on the 20 ppm $^{142}Nd/^{144}Nd$ difference between the Earth and carbonaceous chondrites (Boyet and Carlson, 2005), the primitive mantle would have ε_{Nd} of +7, more depleted than the chondritic Earth value. In this regard, the FOZO could represent the unprocessed, primitive mantle (Jackson et al., 2010; Jackson and Carlson, 2011). However, as reviewed in Section 2, the bulk silicate Earth has a chondritic Sm/Nd ratio.

Different mantle endmembers are also characterized by different major and trace element compositions (Figures 9 and 10). Jackson and Dasgupta (2008) showed that after correction for olivine fractionation, the major element compositions of OIB form linear correlations with isotopic compositions, with HIMU at the low SiO_2 and high CaO end (Figure 9) and EM1, represented by Makapuu-stage Koolau lavas, at the high SiO_2 and low CaO/Al_2O_3 end (Figure 9). EM-type OIB are often characterized by high K_2O content. When comparing with experimental partial melts of eclogite/pyroxenite, Dasgupta et al. (2010) suggested that carbonated SiO_2-poor eclogite contributed to HIMU-type lavas (Kogiso et al., 2003) and volatile-free, SiO_2-rich eclogite contributed to EM1-type lavas (e.g., Hauri, 1996; Lassiter and Hauri, 1998; Huang and Frey, 2005; Sobolev et al., 2005, 2007; Herzberg, 2006, 2014). It is known from experimental petrology that partial melting of the silica-excess eclogite and pyroxenite only produces andesitic to dacitic melts whereas basaltic melts are produced by partial melting of ultramafic lithologies such as

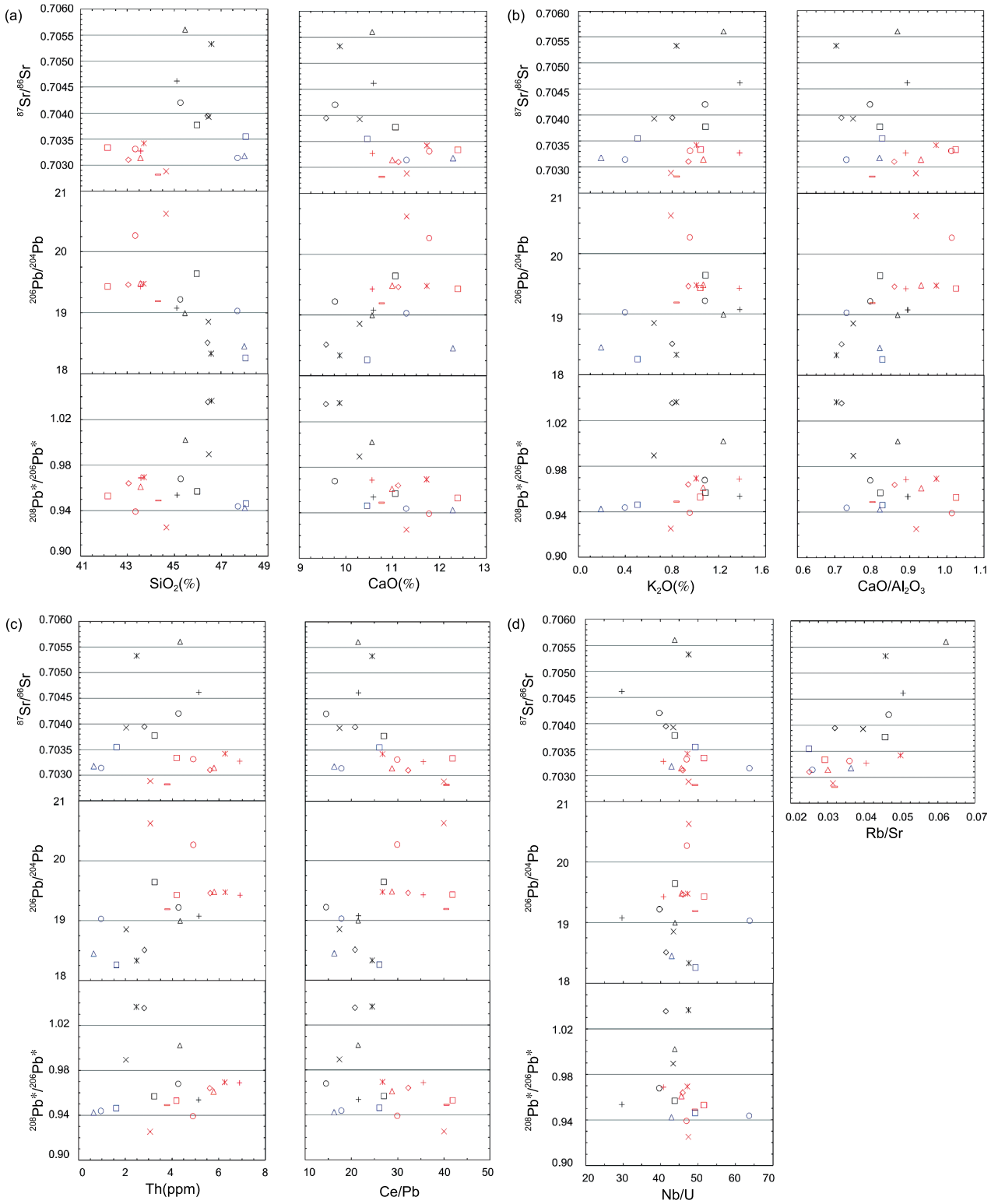

Figure 9 Correlations between chemical compositions and isotopic compositions in OIB averages. Plotted OIBs are the same as that in Figure 6. Only lavas with 8%<MgO<16% are included to minimize the crystal fractionation effects. Data are from GeoRoc data base.

peridotite, silica-decifient pyroxenite and hornblendite. It has been argued that such SiO_2-rich melts would either mix with a picritic melt from peridotite in a magma chamber before eruption (e.g., Hauri, 1996; Jackson et al., 2012), or react with peridotite to form fertile, enriched peridotites (Herzberg et al., 2014) to olivine-free pyroxenites (Sobolev et al., 2005, 2007).

Figure 10 shows the primitive mantle-normalized trace el-

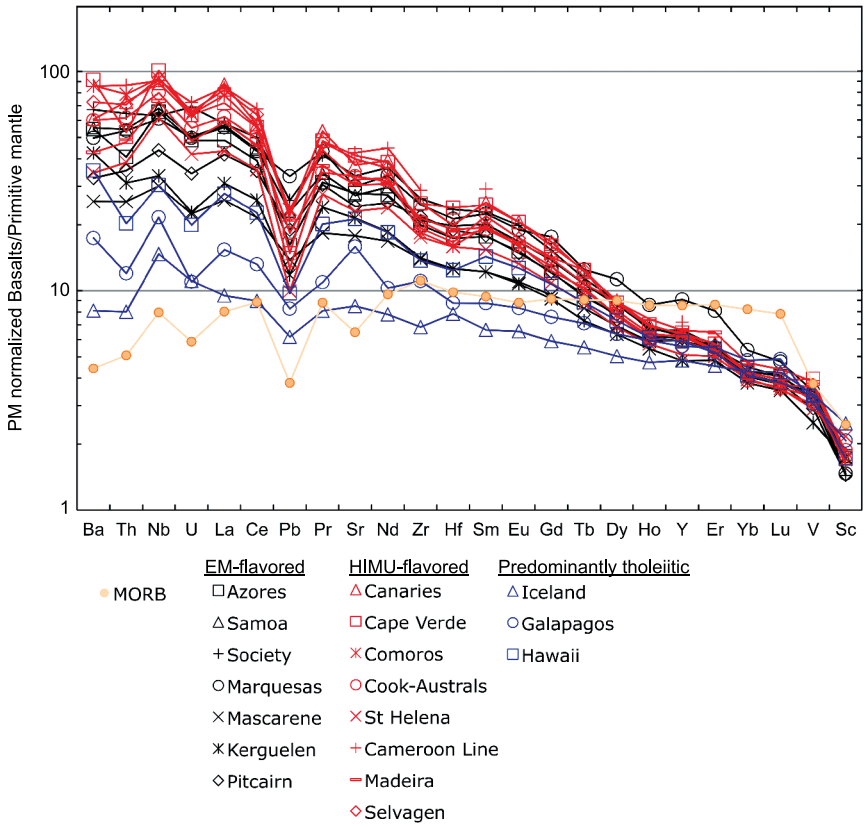

Figure 10 Primitive mantle normalized trace element patterns of OIB averages. Only lavas with 8%<MgO<16% are included to minimize the crystal fractionation effects. Data are from GeoRoc data base and are listed in Table 2. MORB averages are from Gale et al. (2013).

ement patterns for OIB. In order to minimize the crystal fractionation effect, only lavas with 8%<MgO<16% have been used. In contrast to MORB whose highest enrichment is obtained in moderate incompatible elements, the highest enrichment in OIB are achieved in highly incompatible elements, implying a role of crustal components in the OIB mantle sources (Hofmann, 1988). Highly incompatible element contents in all OIB vary by a factor of 10, but HREE-V-Sc by a factor of less than 2. The limited variations in HREE-V-Sc that are compatible in garnet, implying that partial melting of the mantle to produce OIB could have occurred in the garnet stability field (e.g., Hofmann et al., 1984). Alternatively, their mantle sources may be generated by metasomatic reaction of the depleted MORB mantle peridotite with variable amounts of felsic melts derived from partial melting of the subducted oceanic crust in the garnet stability field (Zheng et al., 2015), because such melts are characterized by enrichment in highly incompatible elements and depletion in HREE-V-Sc. This is a crustal metasomatism process to the mantle (Frey and Green, 1974; Zheng, 2012). Recently, Xu et al. (2017) and Xu and Zheng (2017) have provided a quantitative account for the geochemical balance in the origin of OIB-like continental basalts using this model.

In the primitive-mantle normalized diagram (Figure 10), all OIB are characterized by negative U and Pb anomalies. Importantly, in general, Nb/U and Ce/Pb are negatively correlated with $^{87}Sr/^{86}Sr$ in OIB, in which EM-type OIB define the low Nb/U and Ce/Pb but high $^{87}Sr/^{86}Sr$ end (Figure 9). This has been used to argue for a contribution from ancient continental crust component to the EM-type mantle source (e.g., Hofmann et al., 1986; Hofmann, 1997; Jackson et al., 2007; Sun et al., 2008), because continental crust is characterized by low Nb/U and Ce/Pb ratios (Rudnick and Gao, 2003). HIMU-type lavas tend to have higher abundances of highly incompatible elements, thus form steeper trends in Figure 10. This is better shown in a $^{206}Pb/^{204}Pb$ vs. Th plot, in which OIB averages form a positive trend (Figure 9c). This might reflect more of a recycled crustal component in the mantle source of HIMU-type lavas. Finally, OIB averages form a positive Rb/Sr vs. $^{87}Sr/^{86}Sr$ trend (Figure 9d), implying that EM-type mantle sources have higher Rb/Sr. The high K_2O content and high Rb/Sr are often associated with EM-type OIB (Jackson and Dasgupta, 2008), consistent with the suggestion that their mantle sources contained recycled terrigenous materials (e.g. Weaver, 1991). This positive Rb/Sr vs. $^{87}Sr/^{86}Sr$ yields an age of 1.44±0.65 Ga, if treated as an errorchron. Interestingly, the OIB array in a Pb-Pb diagram (Figure 6b) also yields an age of about 2.0 Ga, if interpreted as an errorchron. These ages were interpreted as the average time of mantle homogenization.

5. Mantle heterogeneity: the role of olivine-poor lithologies

Hofmann and White (1982) proposed that recycled oceanic crust is important to the origin of OIB and thus to the composition of mantle plumes. Niu and O'Hara (2003) argued that recycled MORB are too depleted in highly incompatible trace elements such as LILE and LREE to generate the highly incompatible trace element enrichment in OIB. However, recycled oceanic crust includes both underlying basaltic crust and the overlying sediment, and this mixture is able to explain the enrichment of highly incompatible elements in OIB (e.g., Lassiter and Hauri, 1998; Huang and Frey, 2005; Jackson et al., 2007). Under mantle conditions, the bulk subducted MORB is denser than the peridotitic mantle; consequently, they may eventually sink to the core-mantle boundary (e.g., Niu and O'Hara, 2003; Hirose et al., 2005). This has been used to argue against the contribution of a subducted MORB component to mantle plumes (e.g., Niu and O'Hara, 2003). However, this problem can be solved by simply arguing that a mantle plume is a mixture of peridotite and recycled MORB, so that this bulk mixture may be buoyant under higher temperature compared to ambient mantle. Nevertheless, Sun et al. (2011) provided a different solution. In detail, they argued that the subducted MORB at the core-mantle boundary may experience segregation of dense minerals, such as Mg- and Ca-bridgmanites, which increase the SiO_2 content and decrease the density of the subducted MORB until they become buoyant.

Under mantle *P-T* conditions, recycled crustal rocks transform to silica-excess eclogite/garnet pyroxenite. Their partial melts are andesitic to dacitic. Consequently, they cannot be the major component in the OIB mantle source. Although it is now well accepted that recycled ancient slabs are present in the mantle sources of oceanic basalts, it is under debate whether they are sampled in the form of eclogite/garnet pyroxenite in the mantle sources of OIB (Hauri, 1996; Lassiter and Hauri, 1998; Huang and Frey, 2005; Jackson et al., 2012), or eclogite/garnet pyroxenite-derived melts are incorporated into the mantle source of OIB (Sobolev et al., 2005, 2007; Herzberg, 2006; Zhang et al., 2009; Zheng, 2012; Xu et al., 2017).

What happens when a mixture of peridotite and eclogite/garnet pyroxenite partially melts? There are three possible models (Figure 11). The first is magma mixing, in which peridotite and eclogite/garnet pyroxenite are completely isol-

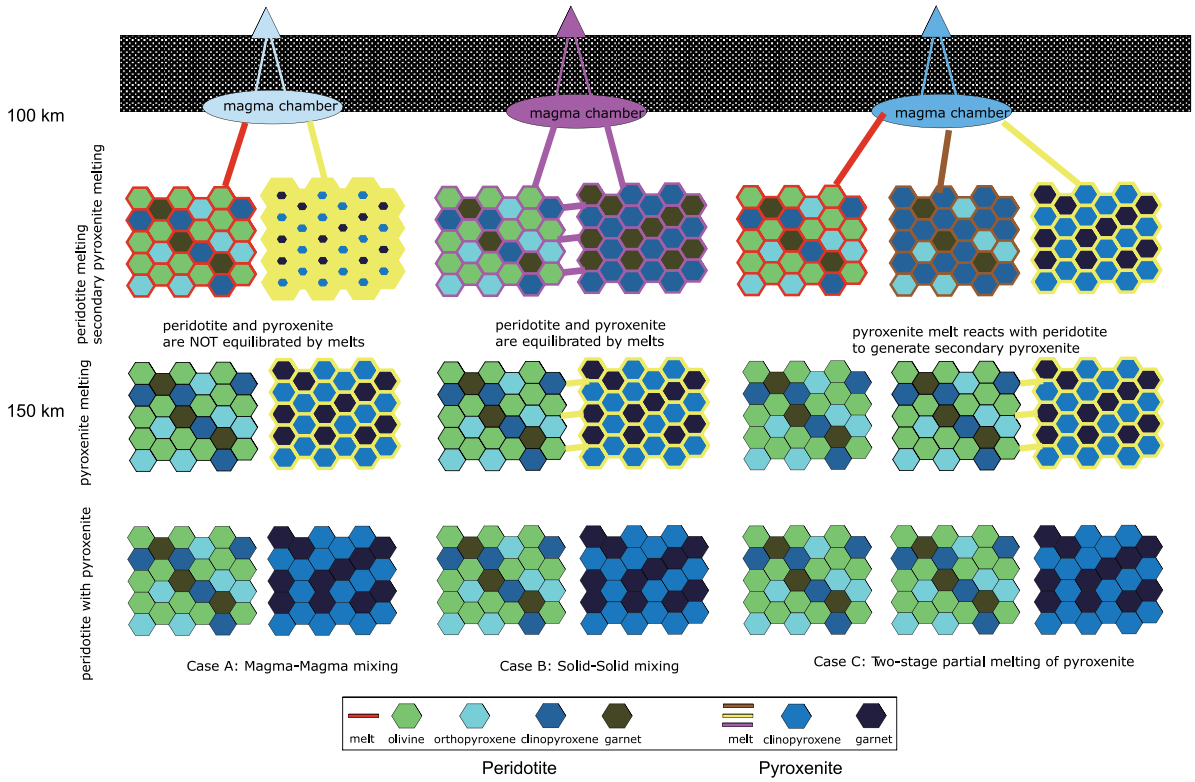

Figure 11 Cartoons showing three possible scenarios for partial melting of a mixture of pyroxenite and peridotite. In case A, pyroxenite and peridotite melt separately, and their magmas do not mix with each other in the mantle. These two magmas flow to the magma chamber separately, and then they mix before eruption. In case B, pyroxenite melts at greater depth, and its melt wets both pyroxenite and peridotie minerals. This process homogenizes both pyroxenite and peridotite, so that this case is equivalent to partial melting a peridotite fertilized by a pyroxenite. Case C describes the two-stage partial melting model, in which the subducted oceanic crust underwent partial melting at first to produce felsic melts, which react with the depleted MORB mantle to generate the metasomatic pyroxenite, whose partial melting gives rise to oceanic island basalts.

ated from each other, and they melt separately to produce basaltic and andesitic-dacitic magmas, respectively. These partial melts make their own way to a shallow magma chamber in which they mix before eruption (Figure 11a). Because of their different solidus temperatures (e.g., Pertermann and Hirschmann, 2003; Lambart et al., 2016), peridotite and eclogite/garnet pyroxenite will melt to different degrees at the same *P*-*T* conditions (e.g., Phipps Morgan, 1999; Stracke and Bourdon, 2009; Lambart et al., 2016). Although eclogite/garnet pyroxenite may melt to a higher degree, the proportion of its SiO_2-rich melt in the erupted magma is also dependent on its proportion in the mixed mantle source. If the mixed mantle source has only a small amount of eclogite/garnet pyroxenite, the erupted magmas are still basaltic (Hauri, 1996; Hirschmann and Stolper, 1996; Lassiter and Hauri, 1998; Huang and Frey, 2005; Jackson et al., 2012).

The second is source mixing. During upwelling, eclogite/garnet pyroxenite may melt first. This melt may percolate through peridotite; consequently, it will homogenize both peridotite and eclogite/garnet pyroxenite. In this case, the eclogite/garnet pyroxenite does not act as an independent lithology. This case is equivalent to basaltic melts originated from relatively homogeneous, enriched peridotites (Figure 11b). Pietruszka et al. (2013) used this model to successfully reproduce the trace element patterns in several Hawaiian volcanoes, Makapuu-stage of Koolau, Mauna Loa, Kilauea, and Loihi.

The third is the two-stage partial melting model, in which peridotite is metasomatized by eclogite/garnet pyroxenite-derived melts at first, and then the ultramafic metasomatites partially melt to generate basaltic magmas (Figure 11c). The melting residue from the first stage may also undergo partial melting at a shallower depth, and contribute to intraplate volcanism (Herzberg, 2006). If the degree of eclogite/garnet pyroxenite melting reaches ~100% in the first stage, this model is equivalent to the second model (Figure 11b). In this case, no enrichment of incompatible trace element occurs in the andesitic-dacitic melts (Xu et al., 2017; Xu and Zheng, 2017).

A role of garnet/garnet pyroxenite in Hawaiian lavas was suggested based on the conflicting inferences from trace elements and major elements. High pressure liquidus experiments on primitive Hawaiian tholeiite compositions show that the major element compositions of Hawaiian tholeiites were equilibrated with a harzbugite residue, and they are too enriched in SiO_2 to be in equilibrium with garnet peridotite (e.g., Green, 1970; Eggins, 1992; Wagner and Grove, 1998). In contrast, a role of residual garnet is inferred for Hawaiian tholeiites based on their relatively constant HREE contents (after correction for olivine fractionation) (e.g., Hofmann et al., 1984; Huang and Frey, 2005). Reaction of the mafic melt with peridotite (Kelemen, 1986) was used to solve this dilemma (Eggins, 1992; Wagner and Grove, 1998; Stolper et al., 2004), in which the primitive Hawaiian magma was first produced by partial melting of garnet peridotite (a kind of fertile, enriched peridotite), then it reacted with a harzburgite (or a sterile, depleted peridotite) on its way up toward the magma chamber. Alternatively, it is argued that silica-excess eclogite/garnet pyroxenite played an important role in generating Hawaiian tholeiites (e.g., Hauri, 1996; Lassiter and Hauri, 1998; Huang and Frey, 2005; Kogiso et al., 2005; Sobolev et al., 2005, 2007; Herzberg, 2006; Jackson et al., 2012). Specifically, Hauri (1996) and Huang and Frey (2005) argued that the eclogite/garnet pyroxenite was sampled as a distinctive lithology (Figure 11a). In this case, andesitic-dacitic melts from eclogite/garnet pyroxenite could mix with basaltic melts from peridotite in a magma chamber before eruption.

Sobolev et al. (2005) proposed the source mixing model in which felsic melts originated from silica-excess eclogite/garnet pyroxenite would react with the peridotite, and replace olivine with pyroxene to form a metasomatic pyroxenite which is characterized by high MgO and Ni contents. Then mafic melt from this pyroxenite would mix with that from peridotite in a magma chamber before eruption (Figure 11b). This model explains the high SiO_2 and high Ni contents in some OIB, especially Hawaiian lavas. Based on CaO contents, Herzberg (2006) even argued that the majority of Hawaiian tholeiites represent mafic melts from this type of metasomatites, and only a small group of lavas with high CaO content are partial melts of peridotites.

The requirement for the involvement of eclogite/garnet pyroxenite in the origin of Hawaiian tholeiites was originally based on geochemical observations, such as high SiO_2 (Hauri, 1996), high Ni (Sobolev et al., 2005, 2007), and low CaO contents (Herzberg, 2006). After taking into account the large Ni variation in peridotites, and a careful reevaluation of the Ni partition coefficient between olivine and basaltic melt (Matzen et al., 2013), it is possible that partial melts from peridotites also have high Ni contents (e.g., Putirka et al., 2011; Rhodes et al., 2012). Similarly, model calculations using BATCH program (Longhi, 2002) suggest that basaltic melts saturated with all four garnet peridotite phases have a large CaO variation (Huang and Humayun, 2016); consequently, a low CaO content cannot be used as a "smoking gun" for the role of eclogite/garnet pyroxenite in generating the mantle source of some OIB, a conclusion also reached by Herzberg et al. (2014).

In addition to SiO_2-rich eclogite/garnet pyroxenite as discussed above, SiO_2-poor (carbonated or not) eclogites/garnet pyroxenites have also been proposed to play a substantial role in OIB petrogenesis, especially for these SiO_2-poor HIMU lavas (e.g., Hirschmann et al., 2003; Kogiso et al., 2003; Keshav et al., 2004; Kogiso and Hirschmann, 2006; Dasgupta et al., 2006, 2010; Lambart et al., 2009; Jackson et al., 2012). While the silica-excess eclogite/garnet pyroxenite are of metamorphic origin, the silica-deficient pyroxenite is

of metasomatic origin. The former serves as the crustal components in the magma sources of oceanic basalts, and its partial melts are felsic with preliminary enrichment in incompatible trace elements. In contrast, the latter serves as the source rocks of some OIB, and its partial melts are mafic with the observed enrichment in incompatible trace elements. Therefore, the two-stage processes are necessary (Figure 11c) in order for OIB to acquire distinctive geochemical signatures like enrichment in highly incompatible trace elements such as LILE and LREE from the subducted oceanic crust (Figure 10). However, the quantitative budget of these trace elements between the subducted MORB and the erupted OIB has raised the problem for physical mixing models (e.g., Niu and O'Hara, 2003). Furthermore, the radiogenic Sr-Nd-Pb isotope compositions of OIB are primarily dictated by those of felsic melts because elements like Sr, Nd and Pb are highly incompatible during crustal anataxis and their abundances in the felsic melts dominate the budget relative to the depleted MORB mantle (Xu and Zheng, 2017).

6. Mantle heterogeneity: recycled crustal signatures in oceanic basalts

There are basically two physical ways to generate mantle heterogeneity: (1) subduction of oceanic and continental lithosphere (Hofmann and White, 1982; Zindler and Hart, 1986; Zheng, 2012), and (2) delamination of lower oceanic and continental crust and their underlying lithospheric mantle (McKenzie and O'Nions, 1983; Anderson, 2005; Lee, 2014). In either case, lithospheric rocks were recycled into the mantle to cause its heterogeneity. Because many crustal and mantle rocks in the recycled lithosphere are susceptible to partial melting in the asthenospheric mantle, felsic to mafic melts are produced at mantle depths to react with the surrounding peridotite. Such reaction can produce fertile, enriched peridotites, a process that was collectively called mantle metasomatism in the literature (e.g., Frey and Green, 1974; Niu and O'Hara, 2003; Donnelly et al., 2004; Workman et al., 2004; O'Reilly and Griffin, 2013).

Zheng (2012) distinguished two types of metasomatism in the mantle. One is the mantle metasomatism whereby the peridotite is metasomatized by mafic melts derived from partial melting of fertile mantle domains. The other is the crustal metasomatism whereby the peridotite is metasomatized by felsic melts derived from partial melting of subducted or delaminated crustal rocks. It appears that the crustal metasomatism denotes the geochemical signatures transferred from the crust to the mantle, which is a primary mechanism for mantle heterogeneity. In contrast, the mantle metasomatism transfers the geochemical signatures from one mantle domain to the other, which is a secondary mechanism for mantle heterogeneity. At converging plate boundaries, crustal materials including sedimentary and magmatic rocks are modified by metamorphic dehydration and partial melting at subduction zone, producing aqueous solutions and hydrous melts that serve as metasomatic agents for crustal metasomatism of the mantle peridotite (Zheng et al., 2016). Once mafic to ultramafic metasomatites are generated in the mantle, they may undergo partial melting to produce mafic melts for mantle metasomatism. Compared to the primitive mantle and residual mantle, therefore, the addition of various metasomatic agents would lead to geochemical and mineralogical heterogeneities, at least for incompatible elements, isotopes and new minerals.

If the crustal rocks were carried into the deep mantle, they contribute to the mantle heterogeneity in both physical and chemical ways. Because the MORB are depleted in highly incompatible trace elements such as LILE and LREE whereas the sediment is enriched in these elements, the physical mixing models for the formation of OIB sources require much more contributions from the sediment than the MORB in order to account for the mass balance between the subducted oceanic crust and the erupted OIB. This is inconsistent with geochemical observations that the majority of OIB share some key trace element signatures with MORB (Hofmann et al., 1986; Sun et al., 2008). This problem can be solved by a chemical mixing model (Zhang et al., 2009; Zheng et al., 2015; Xu et al., 2017), in which the subducted MORB undergo low-degree partial melting, producing felsic melts that are relatively enriched in these trace elements (McKenzie, 1989; Donnelly et al., 2004; Xu et al., 2017). If such melts, together with partial melts from the subducted sediment, react with the depleted MORB mantle, it is able to generate ultramafic metasomatites with considerable enrichment in these highly incompatible trace elements. In doing so, rutile in the subducted oceanic crust broke down and dissolved into the felsic melts, making no depletion or even enrichment of HFSE such as Nb, Ta and Ti in the OIB source (Ringwood, 1990; Prytulak and Elliott, 2007; Jackson et al., 2008; Zheng, 2012; Xu and Zheng, 2017). Therefore, it is possible for the convective mantle to undergo the crustal metasomatism before the subducting slab sinks to the core-mantle boundary.

Recycling of supracrustal material into the mantle has been recognized in OIB. In fact, many OIB show geochemical signatures that can only be produced on the surface of Earth. Lassiter and Hauri (1998) interpreted the high $\delta^{18}O$ values (>5.6‰) in olivines from Makapuu-stage Koolau volcano at Hawaii reported by Eiler et al. (1996) as a result of recycled sediments in the mantle source of Hawaiian basalts. This is based on the knowledge that high $\delta^{18}O$ values can only be generated by low temperature water-rock reaction, where low $\delta^{18}O$ values can only be produced by high temperature water-rock reaction (e.g., Muehlenbachs and Clayton, 1976; Gregory and Taylor, 1981; Eiler, 2001). Olivines from Society and Samoa, all EM2-like, also have high $\delta^{18}O$ values of

5.7–6.0‰ (Eiler et al., 1997; Workman et al., 2008), and they are attributed to recycling of terrigenous material into their mantle sources. Similar arguments have also been made to MORB. Eiler et al. (2000) reported ~0.4‰ δ^{18}O variations in MORB, which are correlated with compositional variations. They argued for a role of the recycled crustal component in the mantle source of MORB. Furthermore, Cooper et al. (2004) observed variable δ^{18}O values (up to 5.6) in MORB glasses from mid-Atlantic ridge, and they preferred a metasomatic model in which the depleted MORB mantle was metasomatized by felsic melts derived from partial melting of a subducted, altered but dehydrated oceanic crust. So did Donnelly et al. (2004) for the trace element systematics in enriched MORB from the mid-Atlantic ridge. Therefore, the high δ^{18}O signatures in both OIB and MORB originated from the supracrustal process. Mineral O isotope homogenization is fast at mantle temperatures (Zheng et al., 2003), so that it is critical to evaluate the timescale for preservation of these supercrustal O isotope signatures in the mantle sources of these oceanic basalts (Zhang et al., 2009).

Farquhar et al. (2000, 2002) reported distinctive mass independent fractionation (MIF) of S isotopes in sulfides and sulfates from crustal rocks older than 2.3 Ga, which disappeared in crustal rocks after 2.0 Ga. This is interpreted to be associated with the great oxygenation event in the Paleoproterozoic. Cabral et al. (2013) reported negative MIF of S isotopes in both olivine sulfide inclusions and bulk olivines from HIMU-type basalts at Mangaia in Austral-Cook islands, and argued for a role of ancient (>2.3 Ga) supracrustal material in their mantle source. A similar observation has also been made on OIB at Pitcairn (Delavault et al., 2016). Thus, it is also important to evaluate how these supercrustal S isotope signatures have survived during crustal and mantle melting.

Compared to silicate Earth, carbonates have light Ca isotopes (e.g., Fantle and Tipper, 2014). Huang et al. (2011a) observed that Hawaii Makapuu-stage Koolau lavas have $\delta^{44/40}$Ca values lower than that of typical upper mantle by 0.3‰, and $\delta^{44/40}$Ca values for Hawaiian lavas are correlated with Sr/Nb and ^{87}Sr/^{86}Sr ratios (Figure 12). They attributed this to a role of recycled carbonates (up to 4%) in the mantle source of Hawaiian lavas. Because of the different element diffusion rates in mantle rocks and melts (e.g., Hofmann and Hart, 1978; Van Orman et al., 2002), kinetic studies may provide insights into the physicochemical mechanism for the preservation of supracrustal signatures in deep mantle.

7. Core-mantle interaction signatures in OIB

Seismic images suggest that some mantle plumes may rise from the core-mantle boundary (Montelli et al., 2004, 2006; French and Romanowicz, 2015). It has also been proposed that mantle plumes may be associated with the LLSVP (large low shear wave velocity province) at the bottom of the mantle (e.g., Hart, 1984; Castillo, 1988; Ni and Helmberger, 2003; He et al., 2015). Furthermore, geochemical zoning was observed in mantle plumes (Abouchami et al., 2005), which may be linked to their relative positions to LLSVPs (Huang et al., 2011b; Weis et al., 2011; Chauvel et al., 2012; Farnetani et al., 2012; Payne et al., 2013; Rohde et al, 2013; Harpp et al., 2014; Jackson et al., 2014; Hoernle et al., 2015; Cordier et al., 2016; but see Jones et al., 2016 for a different point of view). Consistent with this hypothesis, some OIB have distinctive geochemical signatures that may originate from outer core (e.g., Brandon and Walker, 2005), implying a very deep origin.

The Earth's outer core has been argued to have high Pt/Os ratio based on partition coefficients inferred from studies of iron meteorites, so that it has been inferred to have high ^{186}Os/^{188}Os ratios (e.g., Walker et al., 1995; Brandon et al., 1999). High ^{186}Os/^{188}Os ratios observed in Hawaiian picrites (Brandon et al., 1999; Ireland et al., 2011) and Gorgona komatites (Brandon et al., 2003) were interpreted as an outer core signature. However, high-pressure experiments on solid/liquid partitioning of Pt-Re-Os in Fe-S system indicate that solid/liquid partition coefficients of these three elements

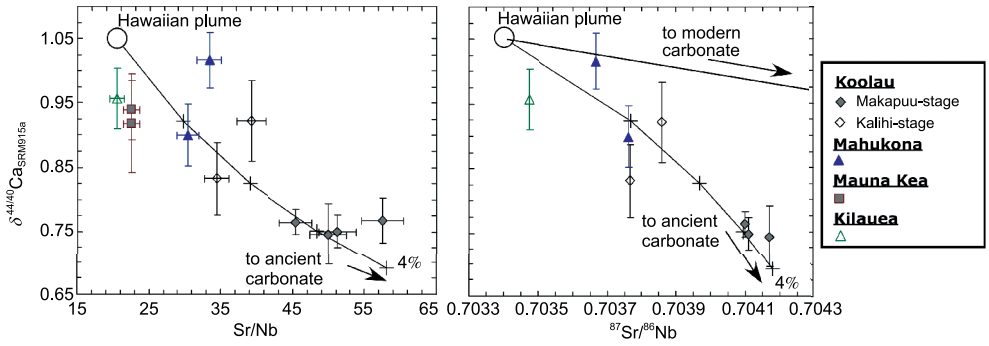

Figure 12 $\delta^{44/40}Ca_{SRM915a}$ vs. Sr/Nb and $^{87}Sr/^{86}Sr$ in Hawaiian tholeiites. These two trends can be reproduced by adding a recycled ancient carbonate component to a plume component. The maximum amount of carbonate added (4%) is labeled at the end of the model mixing lines, and the tick marks represent 1% increments. Mixing line with a modern carbonate forms a shallower $\delta^{44/40}Ca_{SRM915a}$ vs. $^{87}Sr/^{86}Sr$ trend, which cannot explain the Hawaiian trend. Data are from Huang et al. (2011a).

become more similar to each other at high pressure (Van Orman et al., 2008). Consequently, differentiation of the Earth's core is not able to fractionate Pt/Os large enough to explain the observed high $^{186}Os/^{188}Os$ at Hawaii and Gorgona. In addition, Luguet et al. (2008) argued that sulfides from eclogites and pyroxenites have Pt/Os high enough to yield high $^{186}Os/^{188}Os$, if formed early.

Hawaiian tholeiites have Fe/Mn ratios higher than Icelandic lavas and MORB (Figure 13), which was interpreted as an outer core signature (Humayun et al., 2004; Huang et al., 2007; Qin and Humayun, 2008). This interpretation rises because Fe and Mn behavior similarly during partial melting of peridotite, so that a high Fe/Mn ratio in OIB is thought to reflect Fe enrichment in their mantle source that may be caused by the core-mantle interaction. Alternatively, a mantle source with higher fO_2, i.e., higher Fe^{3+}/Fe^{2+}, can also generate high Fe/Mn in the melt, because Fe^{3+} is more incompatible than Fe^{2+}. The fO_2 of primitive Hawaiian lavas is close to the magnetite-wüstite buffer with a Fe^{3+}/total Fe of 0.08 (Rhodes and Vollinger, 2005). For comparison, MORB have a Fe^{3+}/total Fe of 0.12–0.17 (e.g., Bézos and Humler, 2005; Kelley and Cottrell, 2009). Consequently, it is unlikely that the observed high Fe/Mn at Hawaii is the result of a higher fO_2.

As a third option, partial melts of pyroxenite, either silicate-excess or silicate-deficit, are also characterized by high Fe/Mn because Fe is more incompatible than Mn in garnet and pyroxenes (Pertermann and Hirschmann, 2003; Sobolev et al., 2005, 2007). Consequently, it has been suggested that the observed high Fe/Mn in Hawaiian tholeiites (Humayun et al., 2004) can be used to reflect a role of eclogite/garnet pyroxenite in the mantle source of Hawaiian lavas (Sobolev et al., 2005, 2007; Herzberg, 2006). In this case, a correlation is expected to exist between Fe/Mn and olivine fractionation adjusted SiO_2 content (Huang et al., 2007). Nevertheless, the absence of this correlation in the Hawaiian lavas may have different reasons. It is possible that the high Fe/Mn signature at Hawaii would result from partial melting of the metasomatic, secondary garnet pyroxenite. This is because intraplate basalts generally show higher Fe/Mn ratios than MORB, indicating the difference in their source composition.

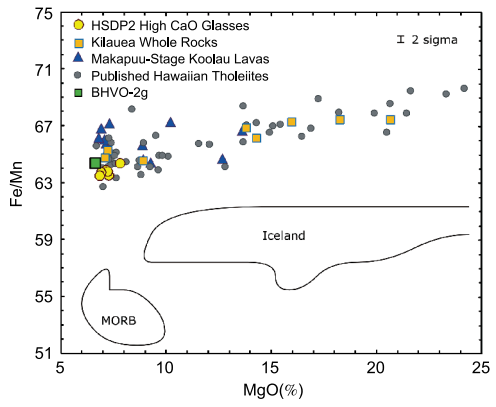

Figure 13 MgO (%) vs. Fe/Mn (wt ratio) in Hawaiian basalts. Fields of MORB and Iceland lavas (Qin and Humayun, 2008) are shown for comparison. Hawaiian lavas are filtered for alteration effect using $1.3<K_2O/P_2O_5<2.0$. Data are from Humayun et al. (2004), Huang et al. (2007), and Huang and Humayun (2016).

In the core-mantle interaction model by Humayun et al. (2004), Fe in the liquid outer core is dissolved back into mantle silicates at the core-mantle boundary. In contrast, Herzberg et al. (2013) proposed a different type of core-mantle interaction, in which silicate mantle and liquid outer core exchange Ni and Fe to cause a Ni enrichment in the reacted mantle. That is, Ni becomes less siderophile at higher temperature (e.g., Fischer et al., 2015). Herzberg et al. (2013) observed high Ni contents, but not high Fe/Mn and low CaO contents, indicators for partial melting of the metasomatic pyroxenite (e.g., Sobolev et al., 2005, 2007; Herzberg, 2006), in petrogenesis of some OIB and large igneous provinces (LIP) including Baffin Island, Ontong Java Plateau, Isla Gorgona and Fernandina at Galapagos. The authors attributed these to the result of core-mantle interaction, implying a very deep origin of their mantle sources. This involves identification of both crustal and mantle metasomatism in the deep mantle, which remains to be resolved in the future.

8. Early-formed, isolated mantle sources: evidence from short-lived nuclides

Short-lived nuclide systems, such as ^{172}Hf to ^{182}W ($t_{1/2}$~9 Myr), ^{146}Sm to ^{142}Nd ($t_{1/2}$~68 or 103 Myr), ^{129}I to ^{129}Xe ($t_{1/2}$~15.7 Myr), and ^{244}Pu to $^{131, 132, 134, 136}Xe$ ($t_{1/2}$ ~80 Myr) that are also produced by ^{238}U, became extinct within the first (up to several) hundred million years of the Earth's history. Isotopic variations involving the daughter products of these short-lived nuclides were produced early in the Earth's history, and any such isotopic variations recorded in terrestrial rocks provide important constraints on the accretion and evolution of Earth (e.g., Jacobsen and Harper, 1996).

In fact, low $\varepsilon^{182}W$ was one of the geochemical signatures proposed for outer core (e.g., Scherstén et al., 2004). ^{182}W is the decay product of the short-lived ^{172}Hf ($t_{1/2}$~9 Myr). Since W is siderophile but not Hf, the Earth's core has a lower Hf/W and hence a lower $\varepsilon^{182}W$ compared to the mantle (Yin et al., 2002; Kleine et al., 2002). The lack of measurable $\varepsilon^{182}W$ in Hawaiian tholeiites that have high $^{186}Os/^{188}Os$ (Walker et al., 1995; Brandon et al., 1999) led Scherstén et al. (2004) to suggest that OIB contain no contribution from the Earth's core. With much improved precision, ±0.05 ε unit compared to >±0.2 ε unit by Scherstén et al. (2004), a recent study reported negative $\varepsilon^{182}W$ data, −0.05 to −0.20, in modern OIBs, including Hawaiian lavas, which are negatively correlated with $^3He/^4He$ (Mundl et al., 2017). They attributed this combined isotopic signature to the entrainment of material from mega-ultralow-velocity zones at the bottom of the mantle, which

may contain metals formed within the first 60 million years after accretion. On the other hand, positive ε^{182}W anomalies have been reported for both ancient and modern rocks (Figure 14), including: 4.0 Ga Acasta gneiss complex in Canada (Willbold et al., 2015), 3.9 Ga supracrustal rocks from the Nuvvuagittuq Greenstone Belt, Quebec, Canada (Touboul et al., 2014), 3.8 Ga rocks from Isua Supracrustal Belt in Greenland (Willbold et al., 2011; Rizo et al., 2016b), 2.8 Ga Kostomuksha komatiites (Touboul et al., 2012), and Phanerozoic flood basalts from Baffin Bay and Ontong Java Plateau (Rizo et al., 2016a). Willbold et al. (2011, 2015) suggest that the high ε^{182}W in early Archean rocks may represent the W isotopic composition of Earth before the arrival of the "late veneer" which controls the modern Earth's platinum group element budget (Day et al., 2016). On the other hand, Touboul et al. (2012) and Rizo et al. (2016a) argued that the positive ε^{182}W anomalies found in much younger 2.8 Ga Kostomuksha komatiites and Phanerozoic flood basalts suggest the preservation of an early formed, within the first hundred million years after Earth accretion, differentiated, with high Hf/W, mantle reservoir until present.

Although no ε^{142}Nd anomaly has been found in modern terrestrial rocks (e.g., Andreasen et al., 2008; Murphy et al., 2010; Cipriani et al., 2011; Jackson and Carlson, 2012; but see also Hyung and Jacobsen, 2016), both positive and negative ε^{142}Nd anomalies have been found in ancient (>2.7 Ga) terrestrial rocks (Figure 15). Harper and Jacobsen (1992) reported ~30 ppm ^{142}Nd excess in 3.8 Ga metasediments from Isua in West Greenland, which was confirmed by a follow-up study reporting 15 ppm ^{142}Nd excess in these rocks (Caro et al., 2003, 2006). It is further shown that high ε^{142}Nd, 10–19 ppm, is a common feature in >3.6 Ga West Greenland rocks (Bennett et al., 2007). Up to 18 ppm ^{142}Nd deficits have been reported in Hadean/Eoarchean mafic and felsic rocks from the Nuvvuagittuq greenstone belt in northern Quebec, Canada (O'Neil et al., 2008, 2012; Roth et al., 2013). Particularly, O'Neil et al. (2012) observed a positively correlated trend between Sm/Nd and ^{142}Nd/^{144}Nd in the Nuvvuagittuq greenstone belt rocks, which, if treated as an isochron, gave an age of 4.4 Ga. In contrast, the Lu-Hf systematics of these rocks yields an age of 3.86±0.07 Ga, consistent with zircon U-Pb ages and whole-rock ^{147}Sm-^{143}Nd dates (Guitreau et al., 2013). Rizo et al. (2012) reported up to 11 ppm ^{142}Nd deficits in 3.4 Ga Ameralik dykes from southwest Greenland. Roth et al. (2014a) reported up to 14 ppm ^{142}Nd deficits in 4.3 Ga Acasta gneiss complex at Canada, which are negatively correlated with positive ε^{182}W anomalies (Willbold et al., 2015). Boyet and Carlson (2005) reported 9–16 ppm ^{142}Nd excess in 2.7–2.9 Ga Belingwe and Kostomuksha komatiites, and Debaille et al. (2013) reported ~7 ppm ^{142}Nd excess in 2.7 Ga Abitibi meta-tholeiites. Upadhyay et al. (2009) reported up to 20 ppm ^{142}Nd deficits in 1.48 Ga Khariar alkaline rocks from southeastern India. However, a subsequent study was not

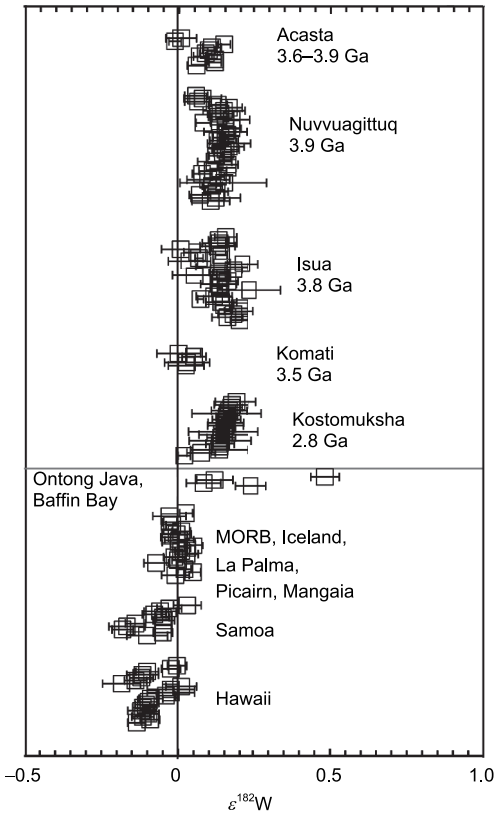

Figure 14 ε^{182}W anomaly in terrestrial rocks. Both negative and positive anomalies are found in modern rocks, but only positive anomalies are reported in ancient rocks (>2.8 Ga). Data are from Willbold et al. (2011, 2015), Touboul et al. (2012, 2014), Rizo et al. (2016a, 2016b), and Mundl et al. (2017).

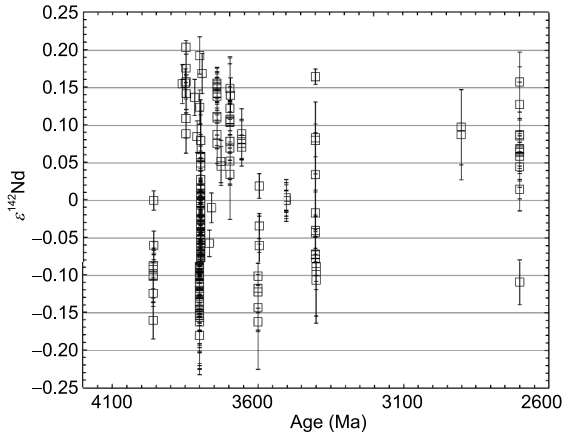

Figure 15 ε^{142}Nd anomaly in terrestrial rocks. Since all published modern rocks do not show measurable ε^{142}Nd anomaly (Andreasen et al., 2008; Murphy et al., 2010; Cipriani et al., 2011; Jackson and Carlson, 2012; but see also Hyung and Jacobsen, 2016), only ancient rocks (>2.7 Ga) are plotted. Compilation of Roth et al. (2014a) are used with data from Caro et al. (2003, 2006), Boyet and Carlson (2005), Bennett et al. (2007), O'Neil et al. (2008, 2012), Rizo et al. (2011, 2012), Roth et al. (2013, 2014a), Debaille et al. (2013).

able to reproduce such a negative anomaly (Roth et al., 2014b). These results evidently imply the early Sm/Nd fractionation in the first hundred million years after Earth formation and its subsequent isolation from mantle convection.

Xenon has nine stable isotopes, 124, 126, 128, 129, 130, 131, 132, 134, and 136, among which ^{129}Xe is the decay product of ^{129}I with $t_{1/2}$ of 15.7 Myr, $^{131, 132, 134, 136}$Xe are produced by spontaneous fission of ^{244}Pu ($t_{1/2}$ ~80 Myr) and ^{238}U, and $^{128, 130}$Xe are primordial. Large and correlated ^{129}Xe/^{130}Xe (2.1–2.7) and ^{136}Xe/^{130}Xe (6.3–7.9) variations have been observed in both MORB and OIB (see Figure 11 of White, 2015; Poreda and Farley, 1992; Kunz et al., 1998; Trieloff et al., 2000; Hopp and Trieloff, 2005; Holland and Ballentine, 2006; Tucker et al., 2012; Parai et al., 2012; Mukhopadhyay, 2012; Pető et al., 2013). The large ^{129}Xe/^{130}Xe and ^{136}Xe/^{130}Xe variations require the early differentiation of I/Xe and Pu/Xe (within the first hundred million years after the Earth accretion) and subsequent preservation of such differentiated mantle reservoirs until present.

Several short-lived isotopic systems, ^{182}Hf-^{182}W, ^{146}Sm-^{142}Nd, ^{129}I-^{129}Xe and ^{244}Pu-^{136}Xe, have been investigated in terrestrial rocks. The observed isotopic anomalies in daughter isotopes require early differentiation events, which must have happened within the first hundred million years after the Earth accretion, and that the early formed differentiated reservoirs must have been preserved for most or all of the Earth's history.

9. Ending remarks

Although our understanding of the Earth's mantle has been greatly advanced in the past several decades, there are still important questions that remain to be solved:

(1) The Earth's mantle is chemically and isotopically heterogeneous, and several mantle reservoirs have been proposed. However, their relationship to mantle structures that are imaged by seismic waves, such as the large low shear wave velocity provinces (LLSVPs) at the bottom of the mantle, is unclear. Ideally, the geochemical pictures of the mantle must be consistent with the geophysical pictures, but geochemical anomalies in the mantle may have much smaller sizes than those imaged by geophysical techniques.

(2) What is role of an olivine-poor lithology, i.e., eclogite/garnet pyroxenite, in the petrogenesis of oceanic basalts? It seems that both peridotite and eclogite/garnet pyroxenite contribute to the formation of oceanic basalts; however, their relative contributions need to be better constrained. It also merits to test whether eclogite/garnet pyroxenite-derived melts dominate the budget of trace elements and their pertinent radiogenic isotopes whereas peridotite dominates the budget of major elements in OIB.

(3) What are the stable isotopic compositions, including both light and metal stable isotopes, of oceanic basalts? Currently, there are only limited data sets, and we feel that it is too early to review them. Nevertheless, it has been shown that stable isotopes are powerful tools to investigate the geochemical kinetics in OIB petrogenesis. In particular, the rate of light element stable isotope (e.g., H, C, O S and N) exchange is much faster than that of heavy element isotopes (e.g., Mg, Ca, Fe, Sr, Nd, Pb, Hf and Os), enabling the estimate of timescales for residence of geochemical anomalies in the mantle.

Acknowledgements *This work was supported by the National Science Foundation (Grant No. NSF EAR-1524387) and National Natural Science Foundation of China (Grant No. 41590620).*

References

Abouchami W, Hofmann A W, Galer S J G, Frey F A, Eisele J, Feigenson M. 2005. Lead isotopes reveal bilateral asymmetry and vertical continuity in the Hawaiian mantle plume. Nature, 434: 851–856

Allègre C J. 1982. Chemical geodynamics. Tectonophysics, 81: 109–132

Armstrong R L. 1968. A model for the evolution of strontium and lead isotopes in a dynamic Earth. Rev Geophys, 6: 175–199

Anders E, Grevesse N. 1989. Abundances of the elements: Meteoritic and solar. Geochim Cosmochim Acta, 53: 197–214

Anderson D L. 2005. Large igneous provinces, delamination, and fertile mantle. Elements, 1: 271–275

Andreasen R, Sharma M. 2006. Solar nebula heterogeneity in p-process samarium and neodymium isotopes. Science, 314: 806–809

Andreasen R, Sharma M, Subbarao K V, Viladkar S G. 2008. Where on Earth is the enriched Hadean reservoir? Earth Planet Sci Lett, 266: 14–28

Barfod D N, Ballentine C J, Halliday A N, Fitton J G. 1999. Noble gases in the Cameroon line and the He, Ne, and Ar isotopic compositions of high μ (HIMU) mantle. J Geophys Res, 104: 29509–29527

Bennett V C, Brandon A D, Nutman A P. 2007. Coupled ^{142}Nd-^{143}Nd isotopic evidence for Hadean mantle dynamics. Science, 318: 1907–1910

Bercovici D, Karato S I. 2003. Whole-mantle convection and the transition-zone water filter. Nature, 425: 39–44

Bézos A, Humler E. 2005. The $Fe^{3+}/\Sigma Fe$ ratios of MORB glasses and their implications for mantle melting. Geochim Cosmochim Acta, 69: 711–725

Birch F. 1952. Elasticity and constitution of the Earth's interior. J Geophys Res, 57: 227–286

Bizimis M, Sen G, Salters V J M, Keshav S. 2005. Hf-Nd-Sr isotope systematics of garnet pyroxenites from Salt Lake Crater, Oahu, Hawaii: Evidence for a depleted component in Hawaiian volcanism. Geochim Cosmochim Acta, 69: 2629–2646

Bizimis M, Salters V J M, Garcia M O, Norman M D. 2013. The composition and distribution of the rejuvenated component across the Hawaiian plume: Hf-Nd-Sr-Pb isotope systematics of Kaula lavas and pyroxenite xenoliths. Geochem Geophys Geosyst, 14: 4458–4478

Blichert-Toft J, Frey F A, Albarède F. 1999. Hf isotope evidence for pelagic sediments in the source of Hawaiian Basalts. Science, 285: 879–882

Blichert-Toft J, White W M. 2001. Hf isotope geochemistry of the Galapagos Islands. Geochem Geophys Geosyst, 2: 1043–2000GC000138

Bouvier A, Boyet M. 2016. Primitive solar system materials and Earth share a common initial ^{142}Nd abundance. Nature, 537: 399–402

Boyet M, Carlson R W. 2005. ^{142}Nd evidence for early (>4.53 Ga) global differentiation of the silicate Earth. Science, 309: 576–581

Brandon A D, Humayun M, Puchtel I S, Leya I, Zolensky M. 2005. Osmium isotope evidence for an s-process carrier in primitive chondrites. Science,

309: 1233–1236
Brandon A D, Norman M D, Walker R J, Morgan J W. 1999. ^{186}Os-^{187}Os systematics of Hawaiian picrites. Earth Planet Sci Lett, 174: 25–42
Brandon A D, Walker R J. 2005. The debate over core-mantle interaction. Earth Planet Sci Lett, 232: 211–225
Brandon A D, Walker R J, Puchtel I S, Becker H, Humayun M, Revillon S. 2003. ^{186}Os-^{187}Os systematics of Gorgona Island komatiites: Implications for early growth of the inner core. Earth Planet Sci Lett, 206: 411–426
Burkhardt C, Borg L E, Brennecka G A, Shollenberger Q R, Dauphas N, Kleine T. 2016. A nucleosynthetic origin for the Earth's anomalous ^{142}Nd composition. Nature, 537: 394–398
Cabral R A, Jackson M G, Rose-Koga E F, Koga K T, Whitehouse M J, Antonelli M A, Farquhar J, Day J M D, Hauri E H. 2013. Anomalous sulphur isotopes in plume lavas reveal deep mantle storage of Archaean crust. Nature, 496: 490–493
Campbell I H, O'Neill H S C. 2012. Evidence against a chondritic Earth. Nature, 483: 553–558
Carlson R W, Boyet M, Horan M. 2007. Chondrite Barium, Neodymium, and Samarium Isotopic heterogeneity and early Earth differentiation. Science, 316: 1175–1178
Caro G, Bourdon B. 2010. Non-chondritic Sm/Nd ratio in the terrestrial planets: Consequences for the geochemical evolution of the mantle-crust system. Geochim Cosmochim Acta, 74: 3333–3349
Caro G, Bourdon B, Birck J L, Moorbath S. 2003. ^{146}Sm-^{142}Nd evidence from Isua metamorphosed sediments for early differentiation of the Earth's mantle. Nature, 423: 428–432
Caro G, Bourdon B, Birck J L, Moorbath S. 2006. High-precision ^{142}Nd/^{144}Nd measurements in terrestrial rocks: Constraints on the early differentiation of the Earth's mantle. Geochim Cosmochim Acta, 70: 164–191
Caro G, Bourdon B, Halliday A N, Quitté G. 2008. Super-chondritic Sm/Nd ratios in Mars, the Earth and the Moon. Nature, 452: 336–339
Castillo P. 1988. The Dupal anomaly as a trace of the upwelling lower mantle. Nature, 336: 667–670
Chauvel C, Hofmann A W, Vidal P. 1992. HIMU-EM: The French Polynesian connection. Earth Planet Sci Lett, 110: 99–119
Chauvel C, Hémond C. 2000. Melting of a complete section of recycled oceanic crust: Trace element and Pb isotopic evidence from Iceland. Geochem Geophys Geosyst, 1: 1001–1999GC000002
Chauvel C, Maury R C, Blais S, Lewin E, Guillou H, Guille G, Rossi P, Gutscher M A. 2012. The size of plume heterogeneities constrained by Marquesas isotopic stripes. Geochem Geophys Geosyst, 13: Q07005
Chen H W, Lee T, Lee D C, Shen J J S, Chen J C. 2011. ^{48}Ca heterogeneity in differentiated meteorites. Astrophys J, 743: L23
Cipriani A, Bonatti E, Carlson R W. 2011. Nonchondritic ^{142}Nd in suboceanic mantle peridotites. Geochem Geophys Geosyst, 12: Q03006
Clayton R N. 2003. Oxygen isotopes in the Solar System. Space Sci Rev, 106: 19–32
Clayton R N, Mayeda T K, Olsen E J, Goswami J N. 1991. Oxygen isotope studies of ordinary chondrites. Geochim Cosmochim Acta, 55: 2317–2337
Clayton R N, Mayeda T K. 1999. Oxygen isotope studies of carbonaceous chondrites. Geochim Cosmochim Acta, 63: 2089–2104
Cooper K M, Eiler J M, Asimow P D, Langmuir C H. 2004. Oxygen isotope evidence for the origin of enriched mantle beneath the mid-Atlantic ridge. Earth Planet Sci Lett, 220: 297–316
Cordier C, Chauvel C, Hémond C. 2016. High-precision lead isotopes and stripy plumes: Revisiting the Society chain in French Polynesia. Geochim Cosmochim Acta, 189: 236–250
Dalton C A, Langmuir C H, Gale A. 2014. Geophysical and geochemical evidence for deep temperature variations beneath mid-ocean ridges. Science, 344: 80–83
Dasgupta R, Hirschmann M M. 2010. The deep carbon cycle and melting in Earth's interior. Earth Planet Sci Lett, 298: 1–13
Dasgupta R, Hirschmann M M, McDonough W F, Spiegelman M, Withers A C. 2009. Trace element partitioning between garnet lherzolite and carbonatite at 6.6 and 8.6 GPa with applications to the geochemistry of the mantle and of mantle-derived melts. Chem Geol, 262: 57–77
Dasgupta R, Hirschmann M M, Stalker K. 2006. Immiscible transition from carbonate-rich to silicate-rich melts in the 3 GPa melting interval of eclogite+CO_2 and genesis of silica-undersaturated ocean island lavas. J Petrol, 47: 647–671
Dasgupta R, Jackson M G, Lee C T A. 2010. Major element chemistry of ocean island basalts—Conditions of mantle melting and heterogeneity of mantle source. Earth Planet Sci Lett, 289: 377–392
Dauphas N, Chen J H, Zhang J, Papanastassiou D A, Davis A M, Travaglio C. 2014. Calcium-48 isotopic anomalies in bulk chondrites and achondrites: Evidence for a uniform isotopic reservoir in the inner protoplanetary disk. Earth Planet Sci Lett, 407: 96–108
Day J M D, Brandon A D, Walker R J. 2016. Highly siderophile elements in Earth, Mars, the Moon, and Asteroids. Rev Mineral Geochem, 81: 161–238
Debaille V, O'Neill C, Brandon A D, Haenecour P, Yin Q Z, Mattielli N, Treiman A H. 2013. Stagnant-lid tectonics in early Earth revealed by ^{142}Nd variations in late Archean rocks. Earth Planet Sci Lett, 373: 83–92
Delavault H, Chauvel C, Thomassot E, Devey C W, Dazas B. 2016. Sulfur and lead isotopic evidence of relic Archean sediments in the Pitcairn mantle plume. Proc Natl Acad Sci USA, 113: 12952–12956
Donnelly K E, Goldstein S L, Langmuir C H, Spiegelman M. 2004. Origin of enriched ocean ridge basalts and implications for mantle dynamics. Earth Planet Sci Lett, 226: 347–366
Drake M J, Righter K. 2002. Determining the composition of the Earth. Nature, 416: 39–44
Dziewonski A M, Anderson D L. 1981. Preliminary reference Earth model. Phys Earth Planet Inter, 25: 297–356
Eggins S M. 1992. Petrogenesis of Hawaiian tholeiites: 1, Phase equilibria constraints. Contrib Mineral Petrol, 110: 387–397
Eiler J M. 2001. Oxygen isotope variations of basaltic lavas and upper mantle rocks. Rev Mineral Geo Chem, 43: 319–364
Eiler J M, Crawford A, Elliott T, Farley K A, Valley J W, Stolper E M. 2000. Oxygen isotope geochemistry of oceanic-arc lavas. J Petrol, 41: 229–256
Eiler J M, Farley K A, Valley J W, Hauri E, Craig H, Hart S R, Stolper E M. 1997. Oxygen isotope variations in ocean island basalt phenocrysts. Geochim Cosmochim Acta, 61: 2281–2293
Eiler J M, Farley K A, Valley J W, Hofmann A W, Stolper E M. 1996. Oxygen isotope constraints on the sources of Hawaiian volcanism. Earth Planet Sci Lett, 144: 453–467
Fantle M S, Tipper E T. 2014. Calcium isotopes in the global biogeochemical Ca cycle: Implications for development of a Ca isotope proxy. Earth-Sci Rev, 129: 148–177
Farley K A, Natland J H, Craig H. 1992. Binary mixing of enriched and undegassed (primitive?) mantle components (He, Sr, Nd, Pb) in Samoan lavas. Earth Planet Sci Lett, 111: 183–199
Farmer GL. 2003. Continental basaltic rocks. Treat Geochem, 3: 85–122
Farnetani C G, Hofmann A W, Class C. 2012. How double volcanic chains sample geochemical anomalies from the lowermost mantle. Earth Planet Sci Lett, 359-360: 240–247
Farquhar J, Bao H, Thiemens M. 2000. Atmospheric influence of Earth's earliest sulfur cycle. Science, 289: 756–758
Farquhar J, Wing B A, McKeegan K D, Harris J W, Cartigny P, Thiemens M H. 2002. Mass-independent sulfur of inclusions in diamond and sulfur recycling on early Earth. Science, 298: 2369–2372
Fischer R A, Nakajima Y, Campbell A J, Frost D J, Harries D, Langenhorst F, Miyajima N, Pollok K, Rubie D C. 2015. High pressure metal-silicate partitioning of Ni, Co, V, Cr, Si, and O. Geochim Cosmochim Acta, 167: 177–194
Fitton J G, Saunders A D, Norry M J, Hardarson B S, Taylor R N. 1997. Thermal and chemical structure of the Iceland plume. Earth Planet Sci

Lett, 153: 197–208
Fitton J G, Saunders A D, Kempton P D, Hardarson B S. 2003. Does depleted mantle form an intrinsic part of the Iceland plume? Geochem Geophys Geosyst, 4: 1032
Foley B J. 2015. The role of plate tectonic-climate coupling and exposed land area in the development of habitable climates on rocky planets. Astrophys J, 812: 36
French S W, Romanowicz B. 2015. Broad plumes rooted at the base of the Earth's mantle beneath major hotspots. Nature, 525: 95–99
Frey F A, Green D H. 1974. The mineralogy, geochemistry and origin of Iherzolite inclusions in Victorian basanites. Geochim Cosmochim Acta, 38: 1023–1059
Frey F A, Huang S, Blichert-Toft J, Regelous M, Boyet M. 2005. Origin of depleted components in basalt related to the Hawaiian hot spot: Evidence from isotopic and incompatible element ratios. Geochem Geophys Geosyst, 6: Q02L07
Frey F A, Huang S, Xu G, Jochum K P. 2016. The geochemical components that distinguish Loa- and Kea-trend Hawaiian shield lavas. Geochim Cosmochim Acta, 185: 160–181
Frey F A, Nobre Silva I G, Huang S, Pringle M S, Meleney P R, Weis D. 2015. Depleted components in the source of hotspot magmas: Evidence from the Ninetyeast Ridge (Kerguelen). Earth Planet Sci Lett, 426: 293–304
Gale A, Dalton C A, Langmuir C H, Su Y, Schilling J G. 2013. The mean composition of ocean ridge basalts. Geochem Geophys Geosyst, 14: 489–518
Gannoun A, Boyet M, Rizo H, El Goresy A. 2011. ^{146}Sm-^{142}Nd systematics measured in enstatite chondrites reveals a heterogeneous distribution of 142Nd in the solar nebula. Proc Natl Acad Sci USA, 108: 7693–7697
Gast P W, Tilton G R, Hedge C. 1964. Isotopic composition of lead and strontium from Ascension and Gough Islands. Science, 145: 1181–1185
Gonnermann H M, Mukhopadhyay S. 2009. Preserving noble gases in a convecting mantle. Nature, 459: 560–563
Gordon R G, Phipps Morgan J. 2016. Recent progress in understanding the origin of the Hawaiian-Emperor Bend. In: American Geophysical Union 2016 Fall Meeting, Abstract GP31D-05
Green D H. 1970. A review of experimental evidence on the origin of basaltic and nephelinitic magmas. Phys Earth Planet Inter, 3: 221–235
Gregory R T, Taylor Jr. H P. 1981. An oxygen isotope profile in a section of Cretaceous oceanic crust, Samail Ophiolite, Oman: Evidence for δ^{18}O buffering of the oceans by deep (>5 km) seawater-hydrothermal circulation at mid-ocean ridges. J Geophys Res, 86: 2737–2755
Guitreau M, Blichert-Toft J, Mojzsis S J, Roth A S G, Bourdon B. 2013. A legacy of Hadean silicate differentiation inferred from Hf isotopes in Eoarchean rocks of the Nuvvuagittuq supracrustal belt (Québec, Canada). Earth Planet Sci Lett, 362: 171–181
Hanan B B, Graham D W. 1996. Lead and helium isotope evidence from oceanic basalts for a common deep source of mantle plumes. Science, 272: 991–995
Hanyu T, Tatsumi Y, Senda R, Miyazaki T, Chang Q, Hirahara Y, Takahashi T, Kawabata H, Suzuki K, Kimura J I, Nakai S. 2011. Geochemical characteristics and origin of the HIMU reservoir: A possible mantle plume source in the lower mantle. Geochem Geophys Geosyst, 12: Q0AC09
Harper C L, Jacobsen S B. 1992. Evidence from coupled ^{147}Sm-^{143}Nd and ^{146}Sm-^{142}Nd systematics for very early (4.5-Gyr) differentiation of the Earth's mantle. Nature, 360: 728–732
Harpp K S, Hall P S, Jackson M G. 2014. Galápagos and Easter: A tale of two hotspots. In: Harpp K S, Mittelstaedt E, d'Ozouville E, Graham D W, eds. The Galápagos: A natural laboratory for the Earth Sciences. 27–40
Hart S R. 1971. The geochemistry of basaltic rocks. Carnegie Institution of Washington Yearbook, 70: 353–355
Hart S R. 1984. A large-scale isotope anomaly in the Southern Hemisphere mantle. Nature, 309: 753–757
Hart S R, Hauri E H, Oschmann L A, Whitehead J A. 1992. Mantle plumes and entrainment: Isotopic evidence. Science, 256: 517–520
Hauri E H. 1996. Major-element variability in the Hawaiian mantle plume. Nature, 382: 415–419
Hauri E H, Hart S R. 1993. ReOs isotope systematics of HIMU and EMII oceanic island basalts from the south Pacific Ocean. Earth Planet Sci Lett, 114: 353–371
Hawkesworth C J, Cawood P A, Dhuime B. 2016. Tectonics and crustal evolution. GSAT, 26: 4–11
He Y, Wen L, Capdeville Y, Zhao L. 2015. Seismic evidence for an Iceland thermo-chemical plume in the Earth's lowermost mantle. Earth Planet Sci Lett, 417: 19–27
Herzberg C. 2006. Petrology and thermal structure of the Hawaiian plume from Mauna Kea volcano. Nature, 444: 605–609
Herzberg C, Asimow P D, Ionov D A, Vidito C, Jackson M G, Geist D. 2013. Nickel and helium evidence for melt above the core-mantle boundary. Nature, 493: 393–397
Herzberg C, Cabral R A, Jackson M G, Vidito C, Day J M D, Hauri E H. 2014. Phantom Archean crust in Mangaia hotspot lavas and the meaning of heterogeneous mantle. Earth Planet Sci Lett, 396: 97–106
Hilton D R, Fischer T P, Marty B. 2002. Noble gases and volatile recycling at subduction zones. Rev Mineral Geochem, 47: 319–370
Hirose K, Takafuji N, Sata N, Ohishi Y. 2005. Phase transition and density of subducted MORB crust in the lower mantle. Earth Planet Sci Lett, 237: 239–251
Hirschmann M M, Kogiso T, Baker M B, Stolper E M. 2003. Alkalic magmas generated by partial melting of garnet pyroxenite. Geology, 31: 481–484
Hirschmann M M, Stolper E M. 1996. A possible role for garnet pyroxenite in the origin of the "garnet signature" in MORB. Contrib Mineral Petrol, 124: 185–208
Hoernle K, Rohde J, Hauff F, Garbe-Schönberg D, Homrighausen S, Werner R, Morgan J P. 2015. How and when plume zonation appeared during the 132 Myr evolution of the Tristan Hotspot. Nat Commun, 6: 7799
Hofmann A W. 1988. Chemical differentiation of the Earth: The relationship between mantle, continental crust, and oceanic crust. Earth Planet Sci Lett, 90: 297–314
Hofmann A W. 1997. Mantle geochemistry: The message from oceanic volcanism. Nature, 385: 219–229
Hofmann AW. 2014. Sampling mantle heterogeneity through oceanic basalts: Isotopes and trace elements. Treatise Geochem, 3: 67–101
Hofmann A W, Feigenson M D, Raczek I. 1984. Case studies on the origin of basalt: III. Petrogenesis of the Mauna Ulu eruption, Kilauea, 1969–1971. Contrib Mineral Petrol, 88: 24–35
Hofmann A W, Hart S R. 1978. An assessment of local and regional isotopic equilibrium in the mantle. Earth Planet Sci Lett, 38: 44–62
Hofmann A W, Jochum K P, Seufert M, White W M. 1986. Nb and Pb in oceanic basalts: New constraints on mantle evolution. Earth Planet Sci Lett, 79: 33–45
Hofmann A W, White W M. 1982. Mantle plumes from ancient oceanic crust. Earth Planet Sci Lett, 57: 421–436
Holland G, Ballentine C J. 2006. Seawater subduction controls the heavy noble gas composition of the mantle. Nature, 441: 186–191
Hopp J, Trieloff M. 2005. Refining the noble gas record of the Réunion mantle plume source: Implications on mantle geochemistry. Earth Planet Sci Lett, 240: 573–588
Huang S, Farkaš J, Jacobsen S B. 2011a. Stable calcium isotopic compositions of Hawaiian shield lavas: Evidence for recycling of ancient marine carbonates into the mantle. Geochim Cosmochim Acta, 75: 4987–4997
Huang S, Farkaš J, Yu G, Petaev M I, Jacobsen S B. 2012. Calcium isotopic ratios and rare earth element abundances in refractory inclusions from the Allende CV3 chondrite. Geochim Cosmochim Acta, 77: 252–265
Huang S, Frey F A. 2005. Recycled oceanic crust in the Hawaiian Plume: Evidence from temporal geochemical variations within the Koolau Shield. Contrib Mineral Petrol, 149: 556–575
Huang S, Humayun M. 2016. Petrogenesis of high-CaO lavas from Mauna

Kea, Hawaii: Constraints from trace element abundances. Geochim Cosmochim Acta, 185: 198–215
Huang S, Humayun M, Frey F A. 2007. Iron/manganese ratio and manganese content in shield lavas from Ko'olau Volcano, Hawai'i. Geochim Cosmochim Acta, 71: 4557–4569
Huang S, Hall P S, Jackson M G. 2011b. Geochemical zoning of volcanic chains associated with Pacific hotspots. Nat Geosci, 4: 874–878
Huang S, Jacobsen S B, Mukhopadhyay S. 2013. ^{147}Sm-^{143}Nd systematics of Earth are inconsistent with a superchondritic Sm/Nd ratio. Proc Natl Acad Sci USA, 110: 4929–4934
Huang S, Lee C T A, Yin Q Z. 2014. Missing lead and high ^{3}He/^{4}He in ancient sulfides associated with continental crust formation. Sci Rep, 4: 5314
Huang S, Jacobsen S B. 2017. Calcium isotopic compositions of chondrites. Geochim Cosmochim Acta, 201: 364–376
Humayun M, Qin L, Norman M D. 2004. Geochemical evidence for excess iron in the mantle beneath Hawaii. Science, 306: 91–94
Hyung E, Huang S, Petaev M I, Jacobsen S B. 2016. Is the mantle chemically stratified? Insights from sound velocity modeling and isotope evolution of an early magma ocean. Earth Planet Sci Lett, 440: 158–168
Hyung E, Jacobsen S B. 2016. ^{142}Nd/^{144}Nd heterogeneity in the proterozoic to phanerozoic mantle and implications for mantle mixing. In: AGU 2016 Fall Meeting DI13B-03
Ireland T J, Walker R J, Brandon A D. 2011. ^{186}Os-^{187}Os systematics of Hawaiian picrites revisited: New insights into Os isotopic variations in ocean island basalts. Geochim Cosmochim Acta, 75: 4456–4475
Jackson M G, Carlson R W. 2011. An ancient recipe for flood-basalt genesis. Nature, 476: 316–319
Jackson M G, Carlson R W. 2012. Homogeneous superchondritic ^{142}Nd/^{144}Nd in the mid-ocean ridge basalt and ocean island basalt mantle. Geochem Geophys Geosyst, 13: Q06011
Jackson M G, Carlson R W, Kurz M D, Kempton P D, Francis D, Blusztajn J. 2010. Evidence for the survival of the oldest terrestrial mantle reservoir. Nature, 466: 853–856
Jackson M G, Dasgupta R. 2008. Compositions of HIMU, EM1, and EM2 from global trends between radiogenic isotopes and major elements in ocean island basalts. Earth Planet Sci Lett, 276: 175–186
Jackson M G, Hart S R, Konter J G, Kurz M D, Blusztajn J, Farley K A. 2014. Helium and lead isotopes reveal the geochemical geometry of the Samoan plume. Nature, 514: 355–358
Jackson M G, Hart S R, Koppers A A P, Staudigel H, Konter J, Blusztajn J, Kurz M, Russell J A. 2007. The return of subducted continental crust in Samoan lavas. Nature, 448: 684–687
Jackson M G, Hart S R, Saal A E, Shimizu N, Kurz M D, Blusztajn J S, Skovgaard A C. 2008. Globally elevated titanium, tantalum, and niobium (TITAN) in ocean island basalts with high ^{3}He/^{4}He. Geochem Geophys Geosyst, 9: Q04027
Jackson M G, Jellinek A M. 2013. Major and trace element composition of the high ^{3}He/^{4}He mantle: Implications for the composition of a nonchonditic Earth. Geochem Geophys Geosyst, 14: 2954–2976
Jackson M G, Konter J G, Becker T W. 2017. Primordial helium entrained by the hottest mantle plumes. Nature, 542: 340–343
Jackson M G, Weis D, Huang S. 2012. Major element variations in Hawaiian shield lavas: Source features and perspectives from global ocean island basalt (OIB) systematics. Geochem Geophys Geosyst, 13: Q09009
Jackson C R M, Parman S W, Kelley S P, Cooper R F. 2013. Noble gas transport into the mantle facilitated by high solubility in amphibole. Nat Geosci, 6: 562–565
Jacobsen S B. 1988. Isotopic constraints on crustal growth and recycling. Earth Planet Sci Lett, 90: 315–329
Jacobsen S B, Harper C L. 1996. Accretion and early differentiation history of the Earth based on extinct radionuclides. Geophys Monograph, 95: 47–74
Jacobsen S B, Wasserburg G J. 1980. Sm-Nd isotopic evolution of chondrites. Earth Planet Sci Lett, 50: 139–155
Jacobsen S B, Wasserburg G J. 1984. Sm-Nd isotopic evolution of chondrites and achondrites, II. Earth Planet Sci Lett, 67: 137–150
Jagoutz E, Palme H, Baddenhausen H, Blum K, Cendales M, Dreibus G, Spettel B, Lorenz V. 1979. The abundances of major, minor and trace elements in the earth's mantle as derived from primitive ultramafic nodules. In: Proceedings of Lunar and Planetary Science Conference, 10. 2031–2050
Jarrard R D. 2003. Subduction fluxes of water, carbon dioxide, chlorine, and potassium. Geochem Geophys Geosyst, 4: 8905–8954
Javoy M, Kaminski E, Guyot F, Andrault D, Sanloup C, Moreira M, Labrosse S, Jambon A, Agrinier P, Davaille A, Jaupart C. 2010. The chemical composition of the Earth: Enstatite chondrite models. Earth Planet Sci Lett, 293: 259–268
Jellinek A M, Jackson M G. 2015. Connections between the bulk composition, geodynamics and habitability of Earth. Nat Geosci, 8: 587–593
Jones T D, Davies D R, Campbell I H, Wilson C R, Kramer S C. 2016. Do mantle plumes preserve the heterogeneous structure of their deep-mantle source? Earth Planet Sci Lett, 434: 10–17
Jungck M H A, Shimamura T, Lugmair G W. 1984. Ca isotope variations in Allende. Geochim Cosmochim Acta, 48: 2651–2658
Kelemen P B. 1986. Assimilation of ultramafic rock in subduction-related magmatic arcs. J Geol, 94: 829–843
Kelley K A, Cottrell E. 2009. Water and the oxidation state of subduction zone magmas. Science, 325: 605–607
Kelley D S, Baross J A, Delaney J R. 2002. Volcanoes, fluids, and life at mid-ocean ridge spreading centers. Annu Rev Earth Planet Sci, 30: 385–491
Keshav S, Gudfinnsson G H, Sen G, Fei Y. 2004. High-pressure melting experiments on garnet clinopyroxenite and the alkalic to tholeiitic transition in ocean-island basalts. Earth Planet Sci Lett, 223: 365–379
Kinoshita N, Paul M, Kashiv Y, Collon P, Deibel C M, DiGiovine B, Greene J P, Henderson D J, Jiang C L, Marley S T, Nakanishi T, Pardo R C, Rehm K E, Robertson D, Scott R, Schmitt C, Tang X D, Vondrasek R, Yokoyama A. 2012. A shorter ^{146}Sm half-life measured and implications for ^{146}Sm-^{142}Nd chronology in the Solar System. Science, 335: 1614–1617
Kleine T, Münker C, Mezger K, Palme H. 2002. Rapid accretion and early core formation on asteroids and the terrestrial planets from Hf-W chronometry. Nature, 418: 952–955
Kogiso T, Hirschmann M M. 2006. Partial melting experiments of bimineralic eclogite and the role of recycled mafic oceanic crust in the genesis of ocean island basalts. Earth Planet Sci Lett, 249: 188–199
Kogiso T, Hirschmann M M, Frost D J. 2003. High-pressure partial melting of garnet pyroxenite: Possible mafic lithologies in the source of ocean island basalts. Earth Planet Sci Lett, 216: 603–617
Kogiso T, Hirschmann M M, Pertermann M. 2005. High-pressure partial melting of mafic lithologies in the mantle. J Petrol, 45: 2407–2422
Korenaga J. 2012. Plate tectonics and planetary habitability: Current status and future challenges. Ann New York Acad Sci, 1260: 87–94
Kunz J, Staudacher T, Allegre C J. 1998. Plutonium-fission xenon found in Earth's mantle. Science, 280: 877–880
Kurz M D, Jenkins W J, Hart S R. 1982. Helium isotopic systematics of oceanic islands and mantle heterogeneity. Naure, 297: 43–47
Kushiro I. 2001. Partial melting experiments on peridotite and origin of mid-ocean ridge basalt. Annu Rev Earth Planet Sci, 29: 71–107
Lambart S, Baker M B, Stolper E M. 2016. The role of pyroxenite in basalt genesis: Melt-PX, a melting parameterization for mantle pyroxenites between 0.9 and 5 GPa. J Geophys Res-Solid Earth, 121: 5708–5735
Lambart S, Laporte D, Schiano P. 2009. An experimental study of pyroxenite partial melts at 1 and 1.5 GPa: Implications for the major-element composition of Mid-Ocean Ridge Basalts. Earth Planet Sci Lett, 288: 335–347
Lassiter J C, Hauri E H. 1998. Osmium-isotope variations in Hawaiian lavas: Evidence for recycled oceanic lithosphere in the Hawaiian plume. Earth Planet Sci Lett, 164: 483–496

Lee C T A. 2014. Physics and chemistry of deep continental crust recycling. Treat Geochem, 4: 423–456
Lee C T A, Luffi P, Höink T, Li J, Dasgupta R, Hernlund J. 2010. Upside-down differentiation and generation of a 'primordial' lower mantle. Nature, 463: 930–933
Lee T, Papanastassiou D A, Wasserburg G J. 1976. Demonstration of ^{26}Mg excess in Allende and evidence for ^{26}Al. Geophys Res Lett, 3: 109–112
Lee T, Papanastassiou D A, Wasserburg G J. 1978. Calcium isotopic anomalies in the Allende meteorite. Astrophys J, 220: L21–L25
Longhi J. 2002. Some phase equilibrium systematics of lherzolite melting: I. Geochem-Geophys-Geosyst, 3: 1–33
Lodders K. 2003. Solar system abundances and condensation temperatures of the elements. Astrophys J, 591: 1220–1247
Luguet A, Graham Pearson D, Nowell G M, Dreher S T, Coggon J A, Spetsius Z V, Parman S W. 2008. Enriched Pt-Re-Os isotope systematics in plume lavas explained by metasomatic sulfides. Science, 319: 453–456
Mansur A T, Manya S, Timpa S, Rudnick R L. 2014. Granulite-facies xenoliths in rift basalts of northern Tanzania: Age, composition and origin of archean lower crust. J Petrol, 55: 1243–1286
Matzen A K, Baker M B, Beckett J R, Stolper E M. 2013. The temperature and pressure dependence of nickel partitioning between olivine and silicate melt. J Petrol, 54: 2521–2545
McDonough W F, Sun S. 1995. The composition of the Earth. Chem Geol, 120: 223–253
McKenzie D. 1989. Some remarks on the movement of small melt fractions in the mantle. Earth Planet Sci Lett, 95: 53–72
McKenzie D, O'Nions R K. 1983. Mantle reservoirs and ocean island basalts. Nature, 301: 229–231
Meissner F, Schmidt-Ott W D, Ziegeler L. 1987. Half-life and α-ray energy of ^{146}Sm. Z Physik A-Atomic Nuclei, 327: 171–174
Montelli R, Nolet G, Dahlen F A, Masters G. 2006. A catalogue of deep mantle plumes: New results from finite-frequency tomography. Geochem Geophys Geosyst, 7: Q11007
Montelli R, Nolet G, Dahlen F A, Masters G, Engdahl E R, Hung S H. 2004. Finite-frequency tomography reveals a variety of plumes in the mantle. Science, 303: 338–343
Morgan W J. 1971. Convection plumes in the lower mantle. Nature, 230: 42–43
Muehlenbachs K, Clayton R N. 1976. Oxygen isotope composition of the oceanic crust and its bearing on seawater. J Geophys Res, 81: 4365–4369
Mukhopadhyay S. 2012. Early differentiation and volatile accretion recorded in deep-mantle neon and xenon. Nature, 486: 101–104
Mundl A, Touboul M, Jackson M G, Day J M D, Kurz M D, Lekic V, Helz R T, Walker R J. 2017. Tungsten-182 heterogeneity in modern ocean island basalts. Science, 356: 66–69
Murakami M, Ohishi Y, Hirao N, Hirose K. 2012. A perovskitic lower mantle inferred from high-pressure, high-temperature sound velocity data. Nature, 485: 90–94
Murphy D T, Brandon A D, Debaille V, Burgess R, Ballentine C. 2010. In search of a hidden long-term isolated sub-chondritic ^{142}Nd/^{144}Nd reservoir in the deep mantle: Implications for the Nd isotope systematics of the Earth. Geochim Cosmochim Acta, 74: 738–750
Newton J, Franchi I A, Pillinger C T. 2000. The oxygen-isotopic record in enstatite meteorites. Meteoritics Planet Sci, 35: 689–698
Ni S, Helmberger D V. 2003. Seismological constraints on the South African superplume; could be the oldest distinct structure on earth. Earth Planet Sci Lett, 206: 119–131
Niederer F R, Papanastassiou D A. 1984. Ca isotopes in refractory inclusions. Geochim Cosmochim Acta, 48: 1279–1293
Niederer F R, Papanastassiou D A, Wasserburg G J. 1985. Absolute isotopic abundances of Ti in meteorites. Geochim Cosmochim Acta, 49: 835–851
Nittler L R, McCoy T J, Clark P E, Murphy M E, Trombka J I, Jarosewich E. 2004. Bulk element compositions of meteorites: A guide for interpreting remote-sensing geochemical measurements of planets and asteroids. Antarctic Meteorite Res, 17: 233–253
Niu Y, O'Hara M J. 2003. Origin of ocean island basalts: A new perspective from petrology, geochemistry, and mineral physics considerations. J Geophys Res, 108: 2209
O'Neil J, Carlson R W, Francis D, Stevenson R K. 2008. Neodymium-142 evidence for Hadean mafic crust. Science, 321: 1828–1831
O'Neil J, Carlson R W, Paquette J L, Francis D. 2012. Formation age and metamorphic history of the Nuvvuagittuq Greenstone Belt. Precambrian Res, 220-221: 23–44
O'Reilly S Y, Griffin W L. 2013. Mantle metasomatism. In: Harlow DE, Austrheim H, eds. Metasomatism and the Chemical Transformation of Rock: The Role of Fluids in Terrestrial and Extraterrestrial Processes. New York: Springer. 471–534
Palme H, Lodders K, Jones A. 2014. Solar System abundances of the elements. In: Davis A M, ed. Ch. 2.2 in Treaties on Geochemistry, 2nd ed. Amsterdam: Elsevier
Palme H, O'Neill H St C. 2014. Cosmochemical estimates of mantle composition. In: Davis A M, ed. Ch. 3.1 in Treaties on Geochemistry, 2nd ed. Amsterdam: Elsevier
Parai R, Mukhopadhyay S, Lassiter J C. 2009. New constraints on the HIMU mantle from neon and helium isotopic compositions of basalts from the Cook-Austral Islands. Earth Planet Sci Lett, 277: 253–261
Parai R, Mukhopadhyay S, Standish J J. 2012. Heterogeneous upper mantle Ne, Ar and Xe isotopic compositions and a possible Dupal noble gas signature recorded in basalts from the Southwest Indian Ridge. Earth Planet Sci Lett, 359-360: 227–239
Parman S W, Kurz M D, Hart S R, Grove T L. 2005. Helium solubility in olivine and implications for high ^{3}He/^{4}He in ocean island basalts. Nature, 437: 1140–1143
Patterson C. 1956. Age of meteorites and the earth. Geochim Cosmochim Acta, 10: 230–237
Payne J A, Jackson M G, Hall P S. 2013. Parallel volcano trends and geochemical asymmetry of the Society Islands hotspot track. Geology, 41: 19–22
Pertermann M, Hirschmann M M. 2003. Partial melting experiments on a MORB-like pyroxenite between 2 and 3 GPa: Constraints on the presence of pyroxenite in basalt source regions from solidus location and melting rate. J Geophys Res, 108: 2125
Pető M K, Mukhopadhyay S, Kelley K A. 2013. Heterogeneities from the first 100 million years recorded in deep mantle noble gases from the Northern Lau Back-arc Basin. Earth Planet Sci Lett, 369-370: 13–23
Phipps Morgan J. 2000. Isotope topology of individual hotspot basalt arrays: Mixing curves or melt extraction trajectories? Geochem Geophys Geosyst, 1: 1003
Pietruszka A J, Norman M D, Garcia M O, Marske J P, Burns D H. 2013. Chemical heterogeneity in the Hawaiian mantle plume from the alteration and dehydration of recycled oceanic crust. Earth Planet Sci Lett, 361: 298–309
Poreda R J, Farley K A. 1992. Rare gases in Samoan xenoliths. Earth Planet Sci Lett, 113: 129–144
Prytulak J, Elliott T. 2007. TiO_2 enrichment in ocean island basalts. Earth Planet Sci Lett, 263: 388–403
Putirka K, Ryerson F J, Perfit M, Ridley W I. 2011. Mineralogy and composition of the oceanic mantle. J Petrol, 52: 279–313
Qin L, Humayun M. 2008. The Fe/Mn ratio in MORB and OIB determined by ICP-MS. Geochim Cosmochim Acta, 72: 1660–1677
Ranen M C, Jacobsen S B. 2006. Barium isotopes in chondritic meteorites: Implications for planetary reservoir models. Science, 314: 809–812
Regelous M, Hofmann A W, Abouchami A, Galer S J G. 2003. Geochemistry of Lavas from the Emperor Seamounts, and the Geochemical Evolution of Hawaiian Magmatism from 85 to 42 Ma. J Petrol, 44: 113–140
Rhodes J M, Huang S, Frey F A, Pringle M, Xu G. 2012. Compositional diversity of Mauna Kea shield lavas recovered by the Hawaii Scientific Drilling Project: Inferences on source lithology, magma supply, and the

role of multiple volcanoes. Geochem Geophys Geosyst, 13: Q03014
Rhodes J M, Vollinger M J. 2005. Ferric/ferrous ratios in 1984 Mauna Loa lavas: A contribution to understanding the oxidation state of Hawaiian magmas. Contrib Mineral Petrol, 149: 666–674
Ringwood A E. 1990. Slab-mantle interactions. ChemGeol, 82: 187–207
Rizo H, Boyet M, Blichert-Toft J, Rosing M. 2011. Combined Nd and Hf isotope evidence for deep-seated source of Isua lavas. Earth Planet Sci Lett, 312: 267–279
Rizo H, Boyet M, Blichert-Toft J, O'Neil J, Rosing M T, Paquette J L. 2012. The elusive Hadean enriched reservoir revealed by ^{142}Nd deficits in Isua Archaean rocks. Nature, 491: 96–100
Rizo H, Walker R J, Carlson R W, Horan M F, Mukhopadhyay S, Manthos V, Francis D, Jackson M G. 2016a. Preservation of Earth-forming events in the tungsten isotopic composition of modern flood basalts. Science, 352: 809–812
Rizo H, Walker R J, Carlson R W, Touboul M, Horan M F, Puchtel I S, Boyet M, Rosing M T. 2016b. Early Earth differentiation investigated through ^{142}Nd, ^{182}W, and highly siderophile element abundances in samples from Isua, Greenland. Geochim Cosmochim Acta, 175: 319–336
Rohde J, Hoernle K, Hauff F, Werner R, O'Connor J, Class C, Garbe-Schonberg D, Jokat W. 2013. 70 Ma chemical zonation of the Tristan-Gough hotspot track. Geology, 41: 335–338
Roth A S G, Bourdon B, Mojzsis S J, Touboul M, Sprung P, Guitreau M, Blichert-Toft J. 2013. Inherited ^{142}Nd anomalies in Eoarchean protoliths. Earth Planet Sci Lett, 361: 50–57
Roth A S G, Bourdon B, Mojzsis S J, Rudge J F, Guitreau M, Blichert-Toft J. 2014a. Combined ^{147,146}Sm-^{143,142}Nd constraints on the longevity and residence time of early terrestrial crust. Geochem Geophys Geosyst, 15: 2329–2345
Roth A S G, Scherer E E, Maden C, Mezger K, Bourdon B. 2014b. Revisiting the ^{142}Nd deficits in the 1.48 Ga Khariar alkaline rocks, India. Chem Geol, 386: 238–248
Rudnick R L, Gao S. 2003. The composition of the continental crust. Treat Geochem, 3: 1–64
Salters V J M, Stracke A. 2004. Composition of the depleted mantle. Geochem Geophys Geosyst, 5: Q05004
Salters V J M, Mallick S, Hart S R, Langmuir C E, Stracke A. 2011. Domains of depleted mantle: New evidence from hafnium and neodymium isotopes. Geochem Geophys Geosyst, 12: Q08001
Scherstén A, Elliott T, Hawkesworth C, Norman M. 2004. Tungsten isotope evidence that mantle plumes contain no contribution from the Earth's core. Nature, 427: 234–237
Schmandt B, Jacobsen S D, Becker T W, Liu Z, Dueker K G. 2014. Dehydration melting at the top of the lower mantle. Science, 344: 1265–1268
Seager S. 2013. Exoplanet habitability. Science, 340: 577–581
Simon J I, DePaolo D J, Moynier F. 2009. Calcium isotope composition of meteorites, earth, and mars. Astrophys J, 702: 707–715
Sleep N H. 1990. Hotspots and mantle plumes: Some phenomenology. J Geophys Res, 95: 6715–6736
Sobolev A V, Hofmann A W, Sobolev S V, Nikogosian I K. 2005. An olivine-free mantle source of Hawaiian shield basalts. Nature, 434: 590–597
Sobolev A V, Hofmann A W, Kuzmin D V, Yaxley G M, Arndt N T, Chung S L, Danyushevsky L V, Elliott T, Frey F A, Garcia M O, Gurenko A A, Kamenetsky V S, Kerr A C, Krivolutskaya N A, Matvienkov V V, Nikogosian I K, Rocholl A, Sigurdsson I A, Sushchevskaya N M, Teklay M. 2007. The amount of recycled crust in sources of mantle-derived melts. Science, 316: 412–417
Stern R J. 2002. Subduction zones. Rev Geophys, 40: 1012
Stolper E, Sherman S, Garcia M, Baker M, Seaman C. 2004. Glass in the submarine section of the HSDP2 drill core, Hilo, Hawaii. Geochem Geophys Geosyst, 5: Q07G15
Stracke A. 2012. Earth's heterogeneous mantle: A product of convection-driven interaction between crust and mantle. Chem Geol, 330-331: 274–299
Stracke A, Bourdon B. 2009. The importance of melt extraction for tracing mantle heterogeneity. Geochim Cosmochim Acta, 73: 218–238
Stracke A, Hofmann A W, Hart S R. 2005. FOZO, HIMU, and the rest of the mantle zoo. Geochem Geophys Geosyst, 6: Q05007, doi:10.1029/2004GC000824
Stuart F M, Lass-Evans S, Godfrey Fitton J, Ellam R M. 2003. High ^{3}He/^{4}He ratios in picritic basalts from Baffin Island and the role of a mixed reservoir in mantle plumes. Nature, 424: 57–59
Sun S S. 1982. Chemical composition and origin of the Earth's primitive mantle. Geochim Cosmochim Acta, 46: 179–192
Sun W, Hu Y, Kamenetsky V S, Eggins S M, Chen M, Arculus R J. 2008. Constancy of Nb/U in the mantle revisited. Geochim Cosmochim Acta, 72: 3542–3549
Sun W, Ding X, Hu Y, Zartman R E, Arculus R J, Kamenetsky V S, Chen M. 2011. The fate of subducted oceanic crust: A mineral segregation model. Int Geol Rev, 53: 879–893
Tang M, Chen K, Rudnick R L. 2016. Archean upper crust transition from mafic to felsic marks the onset of plate tectonics. Science, 351: 372–375
Tarduno J A, Duncan R A, Scholl D W, Cottrell R D, Steinberger B, Thordarson T, Kerr B C, Neal C R, Frey F A, Torii M, Carvallo C. 2003. The emperor seamounts: Southward motion of the hawaiian hotspot plume in Earth's mantle. Science, 301: 1064–1069
Touboul M, Liu J, O'Neil J, Puchtel I S, Walker R J. 2014. New insights into the Hadean mantle revealed by ^{182}W and highly siderophile element abundances of supracrustal rocks from the Nuvvuagittuq Greenstone Belt, Quebec, Canada. Chem Geol, 383: 63–75
Touboul M, Puchtel I S, Walker R J. 2012. ^{182}W evidence for long-term preservation of early mantle differentiation products. Science, 335: 1065–1069
Trieloff M, Kunz J, Clague D A, Harrison D, Allègre C J. 2000. The nature of pristine noble gases in mantle plumes. Science, 288: 1036–1038
Tucker J M, Mukhopadhyay S, Schilling J G. 2012. The heavy noble gas composition of the depleted MORB mantle (DMM) and its implications for the preservation of heterogeneities in the mantle. Earth Planet Sci Lett, 355-356: 244–254
Tucker J M, Mukhopadhyay S. 2014. Evidence for multiple magma ocean outgassing and atmospheric loss episodes from mantle noble gases. Earth Planet Sci Lett, 393: 254–265
Upadhyay D, Scherer E E, Mezger K. 2009. ^{142}Nd evidence for an enriched Hadean reservoir in cratonic roots. Nature, 459: 1118–1121
van der Hilst R D, Widiyantoro S, Engdahl E R. 1997. Evidence for deep mantle circulation from global tomography. Nature, 386: 578–584
Van Orman J A, Grove T L, Shimizu N. 2002. Diffusive fractionation of trace elements during production and transport of melt in Earth's upper mantle. Earth Planet Sci Lett, 198: 93–112
Van Orman J A, Keshav S, Fei Y. 2008. High-pressure solid/liquid partitioning of Os, Re and Pt in the Fe-S system. Earth Planet Sci Lett, 274: 250–257
Vervoort J D, Patchett P J, Blichert-Toft J, Albarède F. 1999. Relationships between Lu-Hf and Sm-Nd isotopic systems in the global sedimentary system. Earth Planet Sci Lett, 168: 79–99
Vervoort J D, Plank T, Prytulak J. 2011. The Hf-Nd isotopic composition of marine sediments. Geochim Cosmochim Acta, 75: 5903–5926
Wagner T P, Grove T L. 1998. Melt/harzburgite reaction in the petrogenesis of tholeiitic magma from Kilauea volcano, Hawaii. Contrib Mineral Petrol, 131: 1–12
Walker R J, Morgan J W, Horan M F. 1995. Osmium-187 enrichment in some plumes: Evidence for core-mantle interaction? Science, 269: 819–822
Weaver B L. 1991. The origin of ocean island basalt end-member compositions: Trace element and isotopic constraints. Earth Planet Sci Lett, 104: 381–397
Weis D, Garcia M O, Rhodes J M, Jellinek M, Scoates J S. 2011. Role of the deep mantle in generating the compositional asymmetry of the Hawaiian mantle plume. Nat Geosci, 4: 831–838

Weiss Y, Class C, Goldstein S L, Hanyu T. 2016. Key new pieces of the HIMU puzzle from olivines and diamond inclusions. Nature, 537: 666–670

White W M. 2015. Isotopes, DUPAL, LLSVPs, and anekantavada. Chem Geol, 419: 10–28

Willbold M, Elliott T, Moorbath S. 2011. The tungsten isotopic composition of the Earth's mantle before the terminal bombardment. Nature, 477: 195–198

Willbold M, Mojzsis S J, Chen H W, Elliott T. 2015. Tungsten isotope composition of the Acasta gneiss complex. Earth Planet Sci Lett, 419: 168–177

Wilson J T. 1963. Evidence from islands on the spreading of ocean floors. Nature, 197: 536–538

Workman R K, Eiler J M, Hart S R, Jackson M G. 2008. Oxygen isotopes in Samoan lavas: Confirmation of continent recycling. Geology, 36: 551–554

Workman R K, Hart S R. 2005. Major and trace element composition of the depleted MORB mantle (DMM). Earth Planet Sci Lett, 231: 53–72

Workman R K, Hart S R, Jackson M, Regelous M, Farley K A, Blusztajn J, Kurz M, Staudigel H. 2004. Recycled metasomatized lithosphere as the origin of the Enriched Mantle II (EM2) end-member: Evidence from the Samoan Volcanic Chain. Geochem Geophys Geosyst, 5: Q04008

Wörner G, Zindler A, Staudigel H, Schmincke H U. 1986. Sr, Nd, and Pb isotope geochemistry of Tertiary and Quaternary alkaline volcanics from West Germany. Earth Planet Sci Lett, 79: 107–119

Xu Z, Zheng Y F. 2017. Continental basalts record the crust-mantle interaction in oceanic subduction channel: A geochemical case study from eastern China. J Asian Earth Sci, 145: 233–259

Xu Z, Zheng Y F, Zhao Z F. 2017. The origin of Cenozoic continental basalts in east-central China: Constrained by linking Pb isotopes to other geochemical variables. Lithos, 268-271: 302–319

Yin Q, Jacobsen S B, Yamashita K, Blichert-Toft J, Télouk P, Albarède F. 2002. A short timescale for terrestrial planet formation from Hf-W chronometry of meteorites. Nature, 418: 949–952

Zeng L, Sasselov D D, Jacobsen S B. 2016. Mass-radius relation for rocky planets based on PREM. Astrophys J, 819: 127

Zhang J, Dauphas N, Davis A M, Leya I, Fedkin A. 2012. The proto-Earth as a significant source of lunar material. Nat Geosci, 5: 251–255

Zhang J J, Zheng Y F, Zhao Z F. 2009. Geochemical evidence for interaction between oceanic crust and lithospheric mantle in the origin of Cenozoic continental basalts in east-central China. Lithos, 110: 305–326

Zhang Y. 2014. Quantification of the elemental incompatibility sequence, and composition of the "superchondritic" mantle. Chem Geol, 369: 12–21

Zhang Z, Stixrude L, Brodholt J. 2013. Elastic properties of $MgSiO_3$-perovskite under lower mantle conditions and the composition of the deep Earth. Earth Planet Sci Lett, 379: 1–12

Zheng Y F. 2012. Metamorphic chemical geodynamics in continental subduction zones. Chem Geol, 328: 5–48

Zheng Y F, Chen Y X, Dai L Q, Zhao Z F. 2015. Developing plate tectonics theory from oceanic subduction zones to collisional orogens. Sci China Earth Sci, 58: 1045–1069

Zheng Y F, Chen R X, Xu Z, Zhang S B. 2016. The transport of water in subduction zones. Sci China Earth Sci, 59: 651–682

Zheng Y F, Chen Y X. 2016. Continental versus oceanic subduction zones. Nat Sci Rev, 3: 651–682

Zheng Y F, Fu B, Gong B, Li L. 2003. Stable isotope geochemistry of ultrahigh pressure metamorphic rocks from the Dabie-Sulu orogen in China: Implications for geodynamics and fluid regime. Earth-Sci Rev, 62: 105–161

Zindler A, Jagoutz E, Goldstein S. 1982. Nd, Sr and Pb isotopic systematics in a three-component mantle: A new perspective. Nature, 298: 519–523

Zindler A, Hart S. 1986. Chemical geodynamics. Annu Rev Earth Planet Sci, 14: 493–571